DANISH METEOROLOGICAL INSTITUTE

SCIENTIFIC REPORT

03-04

Identification of Sources and Long Term Trends for Pollutants in the Arctic Using Isentropic Trajectory Analysis

Alexander Mahura[1,2,5,6] , Dan Jaffe[3,6] and Joyce Harris[4]

[1] Danish Meteorological Institute, DK-2100, Denmark
[2] University of Washington, Atmospheric Sciences Department, WA 98195, USA
[3] University of Washington-Bothell, WA 98021, USA
[4] NOAA, Environmental Research Laboratories, CO 80303, USA
[5] Institute of Northern Environmental Problems, Kola Science Center, Apatity, 184200, Russia
[6] Geophysical Institute, Department of Chemistry, University of Alaska Fairbanks, AK 99775, USA

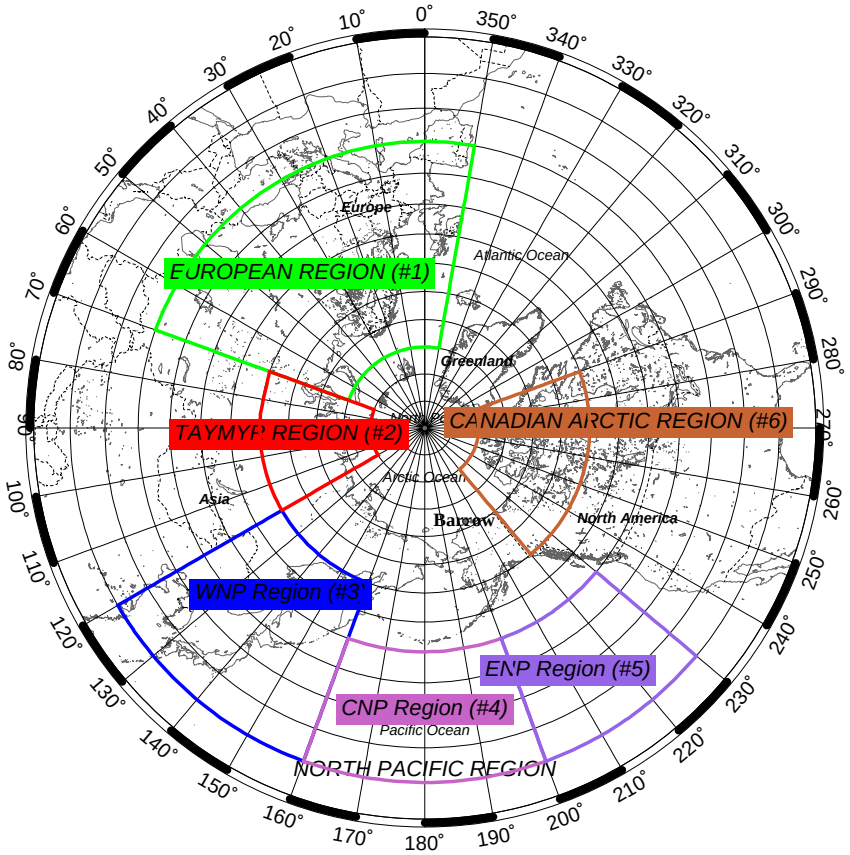

dmi.dk

COPENHAGEN 2003

ISSN: 0905-3263 (printed)
ISSN: 1399-1949 (online)
ISBN: 87-7478-475-7

TABLE OF CONTENTS

FOREWORD 2

EXECUTIVE SUMMARY 3

I. INTRODUCTION 4

II. METHODOLOGY 6

2.1. *ISENTROPIC TRAJECTORY CALCULATIONS* 6

2.2. *SOURCE POLLUTION REGIONS AND SEGREGATION OF TRAJECTORIES* 6

2.3. *CHEMICAL SPECIES RECORDS TREATMENT AND PREPARATION OF DATA SETS FOR ANALYSIS* 7

III. RESULTS AND DISCUSSION 9

3.1. *ATMOSPHERIC TRANSPORT PATTERNS* 9

3.2. *VARIATIONS IN CHEMICAL SPECIES VS SOURCE REGIONS* 12

3.3. *YEAR-TO-YEAR AND MONTH-TO-MONTH VARIATIONS IN FLOW PATTERNS VS CHEMICAL RECORDS* 15

3.4. *ANALYSIS OF ELEVATED CONCENTRATION'S EVENTS FOR AEROSOL SCATTERING COEFFICIENT* 18

3.5. *TWO COMPONENT CORRELATION ANALYSIS* 21

3.6. *INFLUENCE OF THE PRUDHOE BAY INDUSTRIAL AREA ON BARROW'S RECORDS* 24

3.7. *SPECIES' TRENDS BASED ON HOURLY AND FLASK DATA* 26

3.8. *FACTOR ANALYSIS* 31

SUMMARY AND CONCLUSIONS 38

ACKNOWLEDGMENTS 41

REFERENCES 42

FOREWORD

The results of the research project "Identification of Sources and Long Term Trends for Pollutants Using Isentropic Trajectory Analysis" (PIs – Drs. Dan Jaffe and Joyce Harris) - initiated in the University of Alaska, Fairbanks, continued in the University of Washington, and finalized in the Danish Meteorological Institute - are presented in this scientific report. The material of this report was also submitted for a peer-reviewed publication.

In this project, to understand the factors driving climate and ecosystem changes in the Arctic regions we considered sources, correlation and trends for different anthropogenic pollutants. As an example, we selected the NOAA-CMDL Barrow Observatory (Alaska, US) record of pollutant measurements and we applied a set of research tools including trajectory modeling and various statistical analysis techniques.

We assume that results of this study will be useful for current DMI's research projects such as "Arctic Risk" Project of the Nordic Arctic Research Programme (NARP).

Alexander Mahura

EXECUTIVE SUMMARY

The understanding of factors driving climate and ecosystem changes in the Arctic requires careful consideration of the sources, correlation and trends for anthropogenic pollutants. The database from the NOAA-CMDL Barrow Observatory (71°17′N, 156°47′W) is the longest and most complete record of pollutant measurements in the Arctic. It includes observations of carbon dioxide (CO_2), methane (CH_4), carbon monoxide (CO), ozone (O_3), aerosol scattering coefficient (σ_{sp}), aerosol number concentration (NC_{asl}), etc.

The objectives of this study are to understand the role of long-range transport to Barrow in explaining: (1) the year-to-year variations, and (2) the trends in the atmospheric chemistry record at the NOAA-CMDL Barrow observatory. The key questions we try to answer are:

- What is the relationship between various chemical species measured at Barrow Observatory, Alaska and transport pathways at various altitudes?
- What are the trends of species and their relation to transport patterns from the source regions?
- What is the impact of the Prudhoe Bay emissions on the Barrow's records?

To answer on these questions we apply the following main research tools. First, it is an isentropic trajectory model used to calculate the trajectories arriving at Barrow at three altitudes of 0.5, 1.5 and 3 km above sea level. Second - clustering procedure used to divide the trajectories into groups based on source regions. Third - various statistical analysis tools such as the exploratory data analysis, two component correlation analysis, trend analysis, principal components and factor analysis used to identify the relationship between various chemical species vs. source regions as a function of time.

In this study, we used the chemical data from the NOAA-CMDL Barrow observatory in combination with isentropic backward trajectories from gridded ECMWF data to understand the importance of various pollutant source regions on atmospheric composition in the Arctic. We calculated more than 26,000 isentropic backward trajectories arriving at Barrow for a 12-year period (1985-1996) at three elevations (0.5, 1.5 and 3 km). These trajectories had been segregated by source region (European and Taymyr as Eurasian; Eastern, Central and Western North Pacific as North Pacific; and Canadian Arctic), month, season, and year. The chemical data being considered includes methane, carbon dioxide, surface ozone, aerosol number density, aerosol scattering coefficient, and carbon monoxide (flask samples only). Two types of analyses are being performed: relationship between various chemical species and statistical analysis of chemical data segregated by transport pathway.

The clear pattern of the Eurasian region predominance in the transport of the anthropogenic pollutants such as CO, CO_2 and CH_4 was identified and it is in a good agreement with the σ_{sp} data for the same period. The North Pacific region shows the higher concentration of NC_{asl} in comparison with others, which is due to larger contribution of natural than anthropogenic sources. The influence of the Prudhoe Bay industrial area emissions is reflected in the aerosol records: throughout the year the concentration is higher if trajectories arrived from the Prudhoe Bay direction. Factor analysis revealed the existence of the following factors: 1) global hemispheric scale pollution factor (GHSPF) and regional scale pollution factor (RSPF) – which represent the contribution of the carbon and aerosol species throughout the year, and 2) stratospheric ozone intrusions factor (SOIF) – which is reflected only during spring.

I. INTRODUCTION

The understanding of factors driving climate and ecosystem changes in the Arctic requires careful consideration of the sources, correlation and trends for anthropogenic pollutants. The database from the NOAA-CMDL Barrow Observatory (71°17′N, 156°47′W) is the longest and most complete record of pollutant measurements in the Arctic. It includes observations of carbon dioxide (CO_2), methane (CH_4), carbon monoxide (CO), ozone (O_3), aerosol scattering coefficient (σ_{sp}), aerosol number concentration (NC_{asl}), optical depth and black carbon. For some species records go back more than 20 years. To date a large number of the field measurement campaigns have been performed in the Arctic regions including the location of the Barrow site where the continuous measurements of the chemical species are conducted. For Barrow, these studies reflect the analysis of the species' seasonal cycles, possible association with the pollutant source regions, and changes in the species' trends (*Shaw, 1991; Browell et al., 1992; Gregory et al., 1992; Bodhaine and Dutton, 1993; Jaffe et al., 1995; Polissar et al., 1998, Polissar et al., 1999*).

In this study, we used a variety of "data mining" strategies to gain new insight into the Barrow chemical records. The techniques include a variety of statistical methods: exploratory data analysis, simple two component correlation, trend analysis, and multivariate statistical tools such as principal component and factor analysis. We combined chemical data with isentropic trajectories arriving at Barrow for different atmospheric transport regimes. Such analysis may provide insight into the contribution associated with various pollutant source regions. In addition we can use the clustered trajectories to evaluate the differences in pollutant trends and concentrations associated with each individual source region.

For these reasons, we have examined the possibility of the air transport from different geographical source regions to Barrow, Alaska using isentropic trajectories and mentioned above statistical analysis techniques. Goals of this work are to determine:

- the probability and duration of air transport from various source regions to Barrow;
- the temporal (year, seasonal, monthly) and spatial (1.5, 3 and 5 km) distribution of the air transport patterns;
- the source regions responsible for the largest contributions to Arctic pollution;
- the role of variations in the month-to-month and year-to-year flow patterns on the chemical records at Barrow;
- the correlation between various chemical species;

- the long term trends of species and their relation to transport patterns from the source regions;
- the impact of the Prudhoe Bay emissions on the Barrow's records.

In this study we carried out detailed examination of the Barrow datasets including CO_2, CH_4, O_3, and aerosols with respect to the relationship of these species with the isentropic trajectories, interspecies correlation, and trends. Our approach is based on a combined analysis of the isentropic trajectories and the chemical records at Barrow with the different geographical source regions. We studied the atmospheric transport patterns using 10-day backward isentropic trajectories arriving at Barrow during 1985-1996. The role of flow patterns variations vs. species' variations was analyzed by separating the records for each species in time vs. source regions. Correlation between species was identified applying the two component correlation analyses. In this paper we present an analysis using simple statistical tools to evaluate chemical records in combination with trajectories arriving at Barrow. We consider also an analysis of existing trends for species, multivariate statistical analysis tools for various species vs. source regions, and contribution of the local pollution events and Prudhoe Bay emissions on Barrow chemical records.

II. METHODOLOGY

2.1. *ISENTROPIC TRAJECTORY CALCULATIONS*

An atmospheric trajectory determines the most probable history of an air parcel motion over some period of time. It represents the modelled pathway of a parcel advected backward or forward by a wind field in time from a chosen location. Atmospheric trajectory models are very useful to study atmospheric transport pathways and evaluate airflow patterns as well as diagnose a source-receptor relationship for air pollutants (*Miller, 1981; Merrill, 1985; Harris and Kahl, 1990; Harris and Kahl, 1994; Jaffe et al., 1997a; Jaffe et al., 1997b*). The isentropic models use the assumption that an air parcel moves about free of diabatic effects. They ignore radiative transfer, water phase changes as well as mixing of energy/mass. In addition, especially for the Arctic regions, there are complexities and uncertainties due to low resolution of the meteorological data (*Kahl & Samson, 1986; Draxler, 1987*) and trajectory model errors (*Kahl, 1996; Stunder, 1996*). Although such assumptions are inherent in this approach, nevertheless these models are useful research tools.

This study is based on the model developed by *Harris & Kahl, 1994*. The European Center for Medium Range Weather Forecasts (ECMWF) gridded meteorological parameter fields were used as input data for the isentropic trajectory model. The 10-day backward isentropic trajectories were computed twice per day (00 and 12 UTC) at different arrival altitudes of 0.5, 1.5, 3 km above sea level to show variations in the flow patterns for the boundary layer and free troposphere over Barrow. In total, almost 26 thousand trajectories were computed for the period of 1985-1996 (8670 trajectories for 0.5 km, 8647 – 1.5 km and 8682 – 3 km). These trajectories were used to estimate temporal and spatial variability in the airflow patterns and to interpret the chemical species records at Barrow.

2.2. *SOURCE POLLUTION REGIONS AND SEGREGATION OF TRAJECTORIES*

In this study, we originally chose six possible source pollution regions (Figure 1): European, Taymyr, Canadian Arctic and West, Central and East North Pacific Regions. To find, where an air parcel came from, we followed back in time until the trajectory intersected the boundaries of one of the source regions. There we calculated the time of transport and height above sea level as well as assigned trajectory to particular source region. If the trajectory crossed more than one region en-route to Barrow then the trajectory was classified separately and similar parameters were calculated. This was done for all trajectories at each elevation.

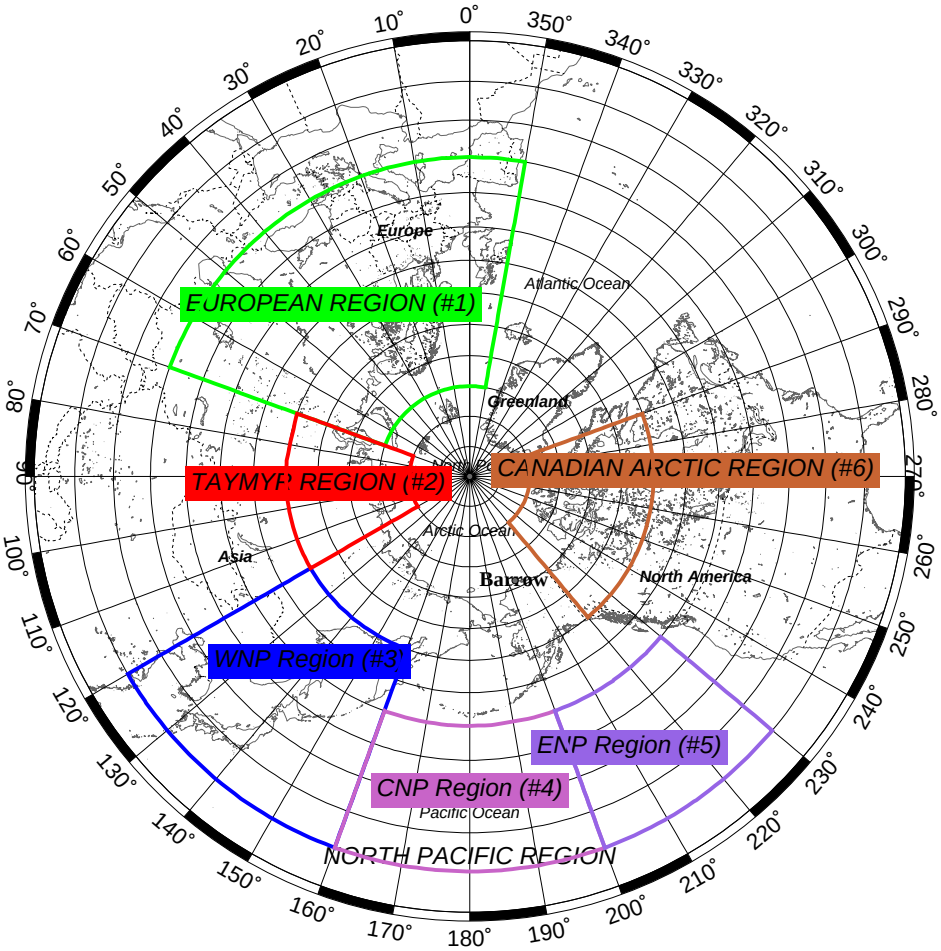

Figure 1. Geographical location of the source regions

2.3. *CHEMICAL SPECIES RECORDS TREATMENT AND PREPARATION OF DATA SETS FOR ANALYSIS*

In this study we used the NOAA CMDL data sets (http://www.cmdl.noaa.gov/info/ftpdata.html) with hourly mixing ratios of CO_2 (ppmv), CH_4 (ppbv), O_3 (ppbv), aerosol scattering coefficient – σ_{sp} (1/m), and aerosol number concentration - NC_{asl} ($1/cm^3$). Only the total light scattering coefficient for the green channel (550 nm) was used because it had the largest percentage of available data. For each of these species we calculated the averages for 00 and 12 UTC using the hourly data at intervals of ±2, ±3, ±6 hours from the midpoint times. Due to the highly skewed nature of NC_{asl} and σ_{sp} distributions the log transformation of these variables were used in our analysis. Three new separate sets were constructed for each species containing averages for the UTC terms for each date where original hourly data were available. The data set using the ±6-h time

interval was chosen for further analysis since the three datasets produced similar results and to incorporate the maximum number of data points.

Combining all sets of individual chemical species, meteorological data and trajectories with source regions, we obtained a set of 7942 records for the period of 1985-1995. Each record contains temporal data (year, month, day, UTC term – 00 or 12, Julian day), information about source regions crossed by the trajectories at three elevations, calculated averages of chemical species and surface wind and velocity. This set named YLP dataset ("yes" local pollution dataset) includes all cases hence reflecting global background, long range transport of species and a possible contribution from local pollution events from the town of Barrow and Prudhoe Bay.

Using the "code flag" from the NOAA CMDL aerosol dataset (code flag shows options - local pollution present or absent) we sorted YLP dataset to build new set – NLP dataset ("no" local pollution dataset) with 4091 records. This dataset presumably excludes local pollution events but still reflects the first two mentioned factors. We re-checked each record using the surface wind velocity and direction and definition of the "clean sector" for Barrow (45-130 degrees). A similar procedure was performed to construct separate datasets for the flask data – CH_4 (ppbv), CO (ppbv), and CO_2 (ppmv) – measured with an average frequency of once per week at Barrow. For these datasets we did not apply any screening to exclude local pollution events.

III. RESULTS AND DISCUSSION

3.1. *ATMOSPHERIC TRANSPORT PATTERNS*

To study the transport patterns to Barrow from the source regions we have examined all 10-day backward trajectories for 1985-1996. For each trajectory where it intersects the relevant source region boundaries we noted the following parameters: the time of transport (in days) and the altitude at the boundary intersection (in m). Each trajectory was assigned to a particular source region. Then statistically we examined trajectories for each source region by month, season and year. In this study we segregated trajectories by source regions to identify main airflow patterns for Barrow. *Harris and Kahl (1994)* used similar approach in the cluster analysis of the trajectories.

The percentage of trajectories, which originated above different individual source regions, is shown in Table 1. The classification "mixed trajectories" was used for cases when trajectories passed through two or three regions on its way to Barrow. The group "no source" includes cases when trajectories do no cross any of the source regions (this group mostly consists of trajectories, which originate over the Arctic Basin and southern areas of the Bering Sea). The percentage of trajectories, originating above the North Pacific regions, increases with altitude but decreases for the northern source regions, except European. This shows that transport of pollution from the industrial European and West North Pacific region possibly occurs at higher altitudes in the comparison with the Taymyr region. Approximately 13.2% of all cases showed, that trajectories had passed two and 1.1% - crossed three regions on the way to Barrow at 0.5 km. The probability of the mixed trajectories increases with altitude reaching almost 26 and 44% at 1.5 and 3 km respectively. The largest number of the mixed trajectories' passages is through the Taymyr-Canadian Arctic, European-Taymyr, West-Central and Central-East Pacific regions. These passages increase transport from the European, Taymyr, West and Central Pacific regions by 1.4-5.1% and 3.6-4.7% at 0.5 and 1.5 km respectively. Such passages might simultaneously carry a "chemical finger print" of more than one source region.

The average transport time to Barrow from each source regions is shown in Table 1. On average an air parcel will travel more than a week to reach Barrow at an altitude of 0.5 km from the European and West North Pacific regions. It will take on average six days for transport from the industrial Taymyr region at all altitudes. The shortest time of transport is from the Canadian Arctic – 3.2 days – due to proximity of the source region to Barrow. The highest probability of transport from the Northern Pacific regions mostly occurs during late spring-summer at all three altitudes and during March at the higher altitudes. It occurs for the European region during June-September and

this probability increases with altitude. The highest occurrence of the transport from the Taymyr region is during November – March at 0.5 km.

Source Region vs. Arrival Height (km)	***No source Reg#0***	***European Reg#1***	***Taymyr Reg#2***	***West North Pacific Reg#3***	***Central North Pacific Reg#4***	***East North Pacific Reg#5***	***Canadian Arctic Reg#6***	***Mixed Traj MT***
	Annual average and inter-annual range of distribution of trajectories (in %)							
0.5	27.5 (23.4-33.7)	1.2 (0-2.6)	11.2 (5.9-16.8)	1.6 (0.3-3.6)	3.6 (1.8-5.5)	2.4 (0.9-6.7)	38.2 (26.8-49.2)	14.3 (10.7-17.3)
1.5	21.7 (18.7-27.3)	1.9 (0.1-4.8)	11.8 (7.1-16.8)	4.7 (2.6-7.9)	5.1 (2.3-7.8)	2.8 (1-6.3)	25.9 (16.4-33.1)	26.1 (20.4-30.5)
3.0	14.7 (10.7-20)	3.4 (1-7.8)	8.0 (5.9-9.9)	6.9 (5.3-9.2)	5.6 (4.2-8.1)	3.0 (1.1-5.8)	14.6 (9.6-18.9)	43.7 (37.3-49.6)
	Average transport time ± 1 standard deviation (in days)							
0.5		7.6±1.6	6.1±2.1	7.3±1.7	6.6±2.1	6.0±2.2	3.2±2.5	
1.5		6.8±2.0	6.1±2.3	6.5±2.0	5.8±2.2	6.0±2.2	3.2±2.5	
3.0		6.0±2.1	6.0±2.3	5.9±2.2	5.6±2.4	5.4±2.4	3.6±2.6	

Table 1. Characteristics of the transport patterns for Barrow at different altitudes for individual source regions.

Source Region vs. Arrival Height (km)	***No Source Reg#0***	***Eurasian Reg#1&2&MT***	***North Pacific Reg#3,4&5&MT***	***Canadian Arctic Reg#6&MT***
Annual average and inter-annual range of distribution of trajectories (in %)				
0.5	27.5 (23.4-33.7)	20.7 (14.2-31)	13.1 (8.6-21.7)	38.7 (27.9-49.5)
1.5	21.7 (18.7-27.3)	26.2 (19.8-33.7)	25.4 (22.1-35.1)	26.6 (17.3-33.5)
3.0	14.7 (10.7-20)	30.1 (21.8-35.5)	39.4 (33.8-44.2)	15.8 (11-19.3)

Table 2. Characteristics of the transport patterns for Barrow at different altitudes for combined source regions.

The individual source regions were re-grouped based on proximity into three categories - Eurasian (transport from the European and Taymyr regions), North Pacific (transport from all three North Pacific regions), and Canadian Arctic regions. All mixed trajectories were re-distributed between three regions based on the trajectory's origin 10 days before arrival at Barrow.

Characteristics of the annual transport patterns for Barrow at different altitudes for combined source regions are shown in Table 2. The monthly distribution of trajectories for these regions is shown in Figure 2, where we calculated the percentage contribution of each combined source region within a month.

Similarities in transport at different elevations provide greater confidence in the transport patterns. We examined the extent to which trajectories calculated at different heights agreed with each other at the same time term (00 and 12 UTC). We found that, on average, only 23.2% of the trajectories, which arrived at Barrow at 0.5 and 1.5 km, originated from the same source region. Only 7.1% of the trajectories came from the same region at all three altitudes. The highest probability for these consistent flow patterns is observed during April (32.2%) at the two lowest altitudes.

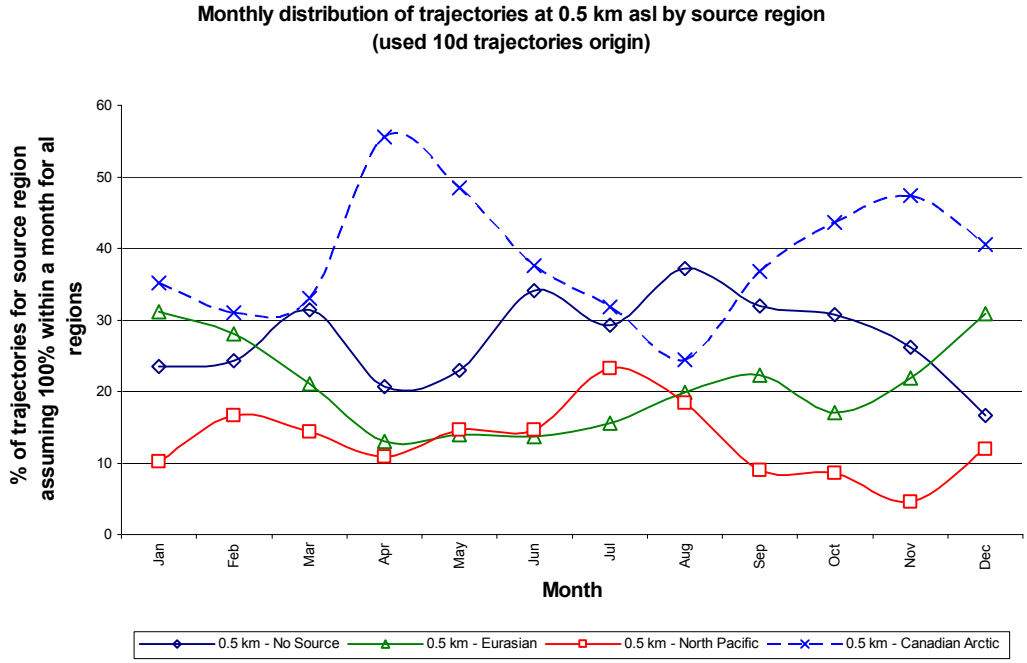

Figure 2. Monthly distribution of trajectories at 0.5 km (used 10-day trajectories origin) based on assumption of % contribution of each combined source region within each month.

Although 10-day trajectories are more useful to indicate possible distant source regions, they do account for an uncertainty of 800-1000 km range after 5 days (*Merrill et al., 1986; Harris, 1994; Dorling and Davies, 1995; Kahl et al., 1996; Stohl, 1998*). Therefore, we also decided to use 5-day trajectories and assign them to different source regions. These 5-day trajectories represent better the main flow patterns to Barrow than show long-range transport from particular remote geographical source region. After screening the total number of trajectories travelling from the Eurasian, North

Pacific and Canadian Arctic regions was reduced by 57, 59 and 17 % at three altitudes respectively. And hence it increased the number of trajectories in the "no source" category. We used both types of trajectories (5 and 10 day) to compare average concentration of chemical species.

3.2. *VARIATIONS IN CHEMICAL SPECIES VS SOURCE REGIONS*

In this study, we looked at differences in the distribution of the species as a function of source region. To identify differences we calculated using NLP dataset monthly averages for probability of transport and concentration of each species for each source region with additional descriptive statistics by month, season, year and entire period. In our study we statistically examined each species vs. source regions, and hence evaluated the contributions to the measured species at Barrow and which geographical regions are "cleaner" and "dirtier". This examination was performed using 5 and 10-day trajectories at 0.5 and 1.5 km altitudes. Table 3 shows annual average concentration, standard deviation and number of used records to estimate statistics for species vs. regions calculated using trajectories with different duration and altitude. One-way ANOVA tests were used to evaluate the statistical significance of the results at 95% confidence level (shown as SS in Table 3) between each source region and "no source".

Although differences in the average concentrations of species between regions are not large we identified several common existing patterns. Firstly, we found that the use of different duration (10 vs. 5 day) as well as trajectory arrival heights does not change the identification of main patterns i.e. which regions are more responsible for contribution of the particular species, except ozone. Secondly, it does not change the occurrence of seasonal minimums and maximums of species for different source regions, but they could be shifted by a month if higher altitude trajectories are considered. Thirdly, for many species, the results are statistically significant at 95% confidence level for the whole year, but there are some months when results are not statistically significant. This occurs more often for σ_{sp} and NC_{asl} in comparison with other species. Fourthly, if 1.5-km trajectories were used the differences in the average concentrations of species between regions are slightly larger and greater statistical significance is observed.

From all used in this study species the σ_{sp} and carbon monoxide are the best indicators of air quality and easily associated with the long-range transport events. This reflects the relatively high emission of densities and contribution from combustion to the global budgets of these species and their relatively moderate lifetimes (e.g. 3-30 days) (*Jaffe et al., 1999*). The highest values for both species are associated with the Eurasian source region.

Source Regions	km	***No Source***			**Eurasian**				***North Pacific***				**Canadian Arctic**				***Barrow (NLP dataset)***		
Chemical Species		Mean	#	StD	Mean	#	StD	SS	Mean	#	StD	SS	Mean	#	StD	SS	Mean	#	StD
CH_4 (ppbv)																			
10-day	0.5	1803.2	846	36.1	1804.66	752	31.7	N	1804.59	405	44.1	N	1796.52	1399	36.9	Y	1801	3402	36.7
10-day	1.5	1801.1	650	40.5	1808.1	869	36.2	Y	1802.69	832	39	N	1793.61	1051	31.1	Y	1801	3402	36.7
CO_2 (ppmv)																			
10-day	0.5	354.73	985	7.2	356.14	807	6.42	Y	355.37	454	7.22	N	355.85	1556	6.54	Y	355.6	3802	6.79
10-day	1.5	354.3	717	7.4	356.07	959	6.55	Y	355.86	955	6.76	Y	355.68	1171	6.54	Y	355.6	3802	6.79
O_3 (ppbv)																			
10-day	0.5	26.05	1016	8.58	27.38	837	8.62	Y	25.11	474	8.56	N	26.94	1625	9.47	Y	26.59	3952	8.99
10-day	1.5	25.3	757	9.13	27.96	973	7.91	Y	26.02	994	8.49	N	26.75	1228	9.9	Y	26.59	3952	8.99
Log CN ($1/cm^3$)																			
10-day	0.5	2.38	1054	0.49	2.33	868	0.43	Y	2.45	489	0.52	Y	2.29	680	0.46	Y	2.34	4091	0.47
10-day	1.5	2.4	777	0.52	2.32	1027	0.46	Y	2.46	1017	0.48	Y	2.22	1270	0.42	Y	2.34	4091	0.47
Log BS (1/m)																			
10-day	0.5	-5.32	1054	0.52	-5.17	868	0.46	Y	-5.37	489	0.52	N	-5.26	1680	0.47	Y	-5.27	4091	0.49
10-day	1.5	-5.36	777	0.51	-5.18	1027	0.49	Y	-5.31	1017	0.51	Y	-5.25	1270	0.46	Y	-5.27	4091	0.49
Flask CO (ppbv)																			
10-day	0.5	139.77	106	40.6	155.19	130	47.2	Y	128.83	51	35.7	N	144.05	145	37.2	N	143.8	402	41.3
10-day	1.5	129.96	71	37.8	154.24	156	44.1	Y	142.15	102	37.8	Y	142.63	108	40.8	Y	143.8	402	41.3

Table 3. Annual average concentration of species by source regions using trajectories arriving at Barrow at different altitudes.

Remarks:

Mean – average concentration of species; # - number of points with 12 hour UTC averages; StD – standard deviation;
SS - statistical significance at 95% confidence level if "no source" and particular source region is compared (Y or N)

A similar pattern is observed for CO_2 and CH_4. Both show higher average values in comparison with other source regions, but the percentage increase is much smaller. For example, compare the average concentration from the Eurasian region with respect to "no source" category gives enhancement of 41, 12, 0.3 and 0.08% for σ_{sp}, CO, CO_2 and CH_4, respectively. This reflects the longer lifetime and larger global reservoirs for CO_2 and CH_4. Also on average globally the anthropogenic contribution of CH_4 is almost as twice larger as from the natural sources. The existence of a long snow cover period in the Eurasian region significantly reduces the amount of CH_4 released by latter. It is well known that during the last decades the increase in CO_2 concentration is mostly attributed to anthropogenic sources. Therefore, on average we have higher concentration of these species associated with anthropogenic sources in the Eurasian region, which is reflected in our dataset. The second largest σ_{sp} values are found for the Canadian Arctic region. The existence of almost similar low concentrations for the North Pacific region as well as "no source" trajectories is explained by occurrence of the large number of trajectories originated over the southern areas of the Bering Sea, and hence possibility of bringing of less industrially polluted air parcels to Barrow.

An intriguing result is found for the North Pacific region, which shows the highest averages for NC_{asl}, but not for σ_{sp} in comparison with other regions. This suggests that these aerosols are probably small and such result could be explained by significant contribution of the natural sources of aerosols. For the North Pacific and Bering Sea regions, there are contributions of natural sources of aerosols: sea salt particles, which are well correlated with the wind, and sulphate particles, as a result of the biogenic phytoplankton activity. Because mostly trajectories pass on a way to Barrow the Bering Sea, which is characterized by high contribution of both mentioned above latter natural sources, we could assume that the contribution of these sources is higher for the North Pacific region in comparison with anthropogenic.

The anthropogenic aerosol's contribution is mostly attributed to the industrialized West and probably East North Pacific regions. For the East North Pacific region such situation could occur if aerosol pollution from the North and Central America sources will be trapped in the boundary layer and then transported to higher latitudes (G.Hakim, UW, personal communication). The relatively low concentration of σ_{sp} from the North Pacific sector suggest that anthropogenic sources adjacent to this area are largely washed out in the North Pacific storm systems prior to being transported to Barrow.

Similar analysis (performed only for 10-day trajectories at both altitudes) of the flask data for CH_4, CO and CO_2 showed similar patterns on a yearly basis as NLP dataset constructed using hourly measurements of species. The European region reflects the higher concentration for all mentioned above species at Barrow in comparison with other source regions. But we should note that these results in common have more number of the months when results are not statistically significant in comparison with NLP dataset. Particular, during September-October tests showed that results are not statistically significant for all source regions. This discrepancy is mostly due to smaller number of flask measurement data points used to perform testing.

Separately we considered the situations when 10-day trajectories at both lower altitudes (0.5 and 1.5 km) showed transport from the same and different source regions at a particular term – "similar trajectories" vs. "dissimilar trajectories" cases (ST vs. DT cases). From the same NLP dataset we calculated the average species concentrations for both cases. In particular, for the NLP dataset the average number of ST vs. DT cases for all species was approximately 33 vs. 77% respectively. From all ST cases, the distribution of cases between source regions was 17, 20, 15, and 48% for the "no source", Eurasian, North Pacific and Canadian Arctic regions, respectively. The following two findings should be mentioned. First, we found that on average on a yearly basis the concentration of species is slightly higher for the ST case. Second, the similar pattern of the Eurasian region predominance is underlined in both ST and DT.

3.3. *YEAR-TO-YEAR AND MONTH-TO-MONTH VARIATIONS IN FLOW PATTERNS VS CHEMICAL RECORDS*

In our study a well-defined seasonal cycle was identified for all species and they are in a good agreement with the previously reported for Barrow (*Oltmans and Levy, 1994; Conway et al., 1994; Dlugokencky et al., 1994; Dlugokencky et al., 1995; Oechel et al., 1995; Bodhaime, 1995*). To evaluate influence of the flow patterns on the distribution of the chemical species concentrations we calculated monthly and yearly averages for species and flow patterns for each source region and then analyzed the constructed time series.

In this study originally we hypothesized that the year-to-year variability in the flow patterns from the different geographical source regions will be reflected in the chemical data records at Barrow. It seemed likely for us that changes in the synoptic patterns from one year to another could also partially explain why some of the years "dirtier" in comparison with others. To test this assumption we estimated year-to-year changes in the concentrations of species and in the

percentage of trajectories arrived at Barrow from different source regions using NLP dataset. In particular, we had interest in the estimation of signs and magnitudes of such changes. We should report that we did not identify a clear dependence of variations in flow patterns to concentration in species.

Some peculiarities in seasonal cycles for chemical species by source regions should be mentioned.

For NC_{asl}, σ_{sp}, O_3 and CO_2 the similar seasonal cycles were identified for source regions as previously reported for the Barrow (*Oltmans and Levy, 1994; Conway et al., 1994; Dlugokencky et al., 1994; Dlugokencky et al., 1995; Oechel et al., 1995; Bodhaime, 1995*). Some differences we identified in the temporal occurrence of the seasonal maximums and minimums throughout the year for some source regions. For CO_2 there is the second relatively flat minimum during February-March only for the North Pacific region. This reflect results of the most winter and spring studies showing that during this time the level of anthropogenic pollutants associated with the transport from the Eurasian region is higher, and we should note that this pattern is observed at both altitudes.

For σ_{sp} we identified well-pronounced first maximum during March for all source regions without exception which is attributed to the period of the Arctic haze. The minimum is observed during June for all regions except the Eurasian region where it occurred one month later. In fact, such shift could be explained by highest contribution of precipitation (21 mm at Barrow) throughout the year within the Arctic territories in comparison with other months.

For NC_{asl} there is a well-defined seasonal cycle with two maximums and minimums. The first maximum (smaller in the absolute magnitude) is observed during early spring Arctic haze (March). Although both the North Pacific and Canadian Arctic trajectories show the higher NC_{asl} during March, the Eurasian trajectories reflect the existence of the "flat" maximum during longer period of time – February-April (when shorter duration trajectories are considered). The second maximum is observed during July for the Eurasian and North Pacific, and it shifted to August for the Canadian Arctic region.

For ozone there is a well-defined seasonal cycle with two maximums and minimums for the Canadian and North Pacific regions. During spring the major source of ozone in the Arctic is the intrusion from the stratosphere. During winter ozone is transported from the industrialized regions in the northern latitudes and photochemistry does not play significant source's role (*Gregory et al., 1992*). Throughout the year transport from the Canadian Arctic are positively correlated with O_3 mixing ratio, except during April-June. Trajectories arriving from the North Pacific region show

two relatively flat minimums almost similar in magnitude during March-April and July-August. The Eurasian region is characterized by minimum in April, and then O_3 steadily increases with some lowering of the rate of this increase during summer months instead of the second minimum as observed for all other regions. Month-to-month flow changes for this region are well positively correlated to O_3 mixing ratio. In particular, during November-April the probability of the transport decreases, and it is accompanied by decrease of concentration. During April-September a gradual increase in the airflow increases O_3 mixing ratio, and finally later this increase slows down in October when the less flow is coming from the region. We should note that there is an interesting pattern for ozone: during January-May the North Pacific region shows on average the higher mixing ratios in comparison with the Eurasian region. Then this situation changes to opposite during June-December. Such pattern is observed also if 1.5 km trajectories are applied.

The most interesting results are for CH_4 (Figure 3). The first well pronounced maximum is observed during March and minimum in June for all source regions. The interesting finding should be mentioned: the North Pacific region shows an occurrence of double adjacent maximums during August and October. The similar pattern is observed for the "no source" category. Similarity between the North Pacific and "no source" might be explained by the fact, that during fall most of the trajectories from the "no source" category have origin above the southern territories of the Bering Sea. The explanation of double maximums supposedly lies in the following. First, we found that during fall the probability of transport is larger at higher elevations from the North Pacific regions. Second, we speculate that the important CH_4 sources for the North Pacific regions are more natural origin than anthropogenic, i.e. possibly have the oceanic origin. This might be valid especially for the Central and East North Pacific regions; but the anthropogenic sources of CH_4 play more important role for the West North Pacific region. Independent check of monthly average CH_4 concentrations for all three North Pacific regions separately showed that only the Central and East North Pacific regions have same pattern of double maximums, but not the West. The occurrence of the sharp intermediate minimum during September is due to sharp decrease (almost by factor of 6) in comparison with the previous month in the transport from the industrial West North Pacific region. September also represents the month with the lowest probability of transport throughout the year for this region (less than half of percent from all trajectories during this month). Therefore, less CH_4 due to anthropogenic sources would be transported toward the Arctic territories and natural sources will play more important role. On a year-to-year basis during these months the double

maximums pattern is observed mostly in the cases when transport from the North Pacific regions has increased in the same time of the year.

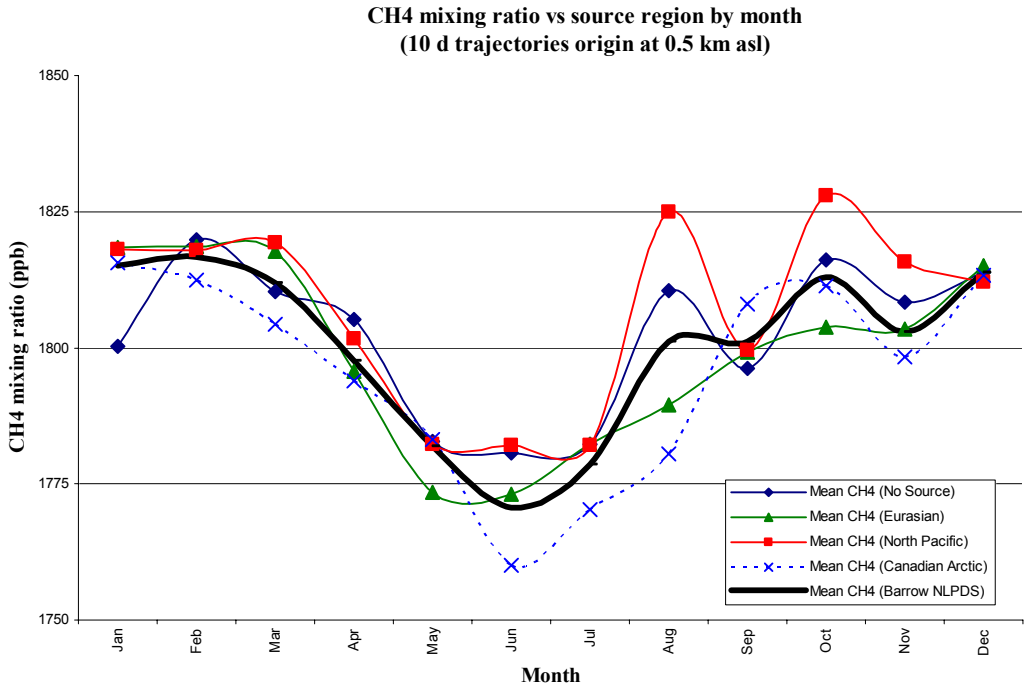

Figure 3. Monthly average CH_4 mixing ratio vs. source regions using 10-day trajectories at 0.5 km.

Also we should mention the controversial monthly distribution with the yearly. On average, there is the higher yearly CH_4 concentration pattern for the Eurasian region (as we mentioned in Table 3), but the lower monthly average as shown at Figure 3. Such result is explained by the existence of the higher (almost by factor of two) standard deviations for the North Pacific region during these months in comparison with the Eurasian region.

3.4. *ANALYSIS OF ELEVATED CONCENTRATION'S EVENTS FOR AEROSOL SCATTERING COEFFICIENT*

As we mentioned previously the σ_{sp} is a good indicator of a relation to the remote source regions due to shorter residence time and hence conveniently could be used to interpret the occurrence of the "specific events" (i.e. cases when the elevated concentrations are recorded). For such events the 10-day trajectories play a better role in identification of the areas of an air parcels' origin. We should note, that large number of the previous studies was focused on these specific events (*Bridgman et al., 1989; Li et al., 1990; Sturges et al., 1993; Bridgman and Bodhaine, 1994; Zaizen et al., 1998*). In particular, during spring, which is well known as the Arctic haze the

pollution mainly comes from the anthropogenic sources in the Eurasian continent. Hence, these studies looked on the identification of the Eurasian sources. In our study we also assumed to consider the Canadian Arctic region as the potential "intermediate" source region. We assumed that originally pollution could arrive from another geographical area and then transported through this region finally reaching the Barrow.

We evaluated top (elevated events – polluted air) and low (lowered events – clean air) 10% of σ_{sp} data by source regions for each month using 10-day trajectories at both altitudes of 0.5 and 1.5 km. It should be noted that up to 30% of all elevated events are related to the "no source" category, and hence were not attributed to any possible source region which left us with the rest 70% to be evaluated. We found that throughout the year the contribution of the Canadian Arctic into the higher top 10% of σ_{sp} data is on average 43% from all elevated events if 0.5-km trajectories are used for interpretation. For this region it has a maximum of 60% in January. For the Eurasian region, the probability of such elevated events is on average of 18% throughout the year. It is the highest (36%) during winter and early spring and the lowest of 7.4 and 6.9% during June-July, respectively. This lower occurrence for the Eurasian region during summer could be explained by the significant influence of the precipitation during transport. The North Pacific region is characterized by the lowest occurrence of the elevated events. On average it is less than 10% throughout the year. But during June-July this probability raises up to 19 and 31% respectively. This output changes if we consider 1.5-km trajectories for the interpretation of the elevated events. On average the occurrence of such elevated events increases for the Eurasian region up to 25% and almost by factor of 3 for the North Pacific region. We should note that summer keeps the same pattern as at 0.5 km .

The possible explanation of the elevated events' occurrence from the Canadian Arctic region could be the following. Inspection of trajectories shows that on a way to pass the Canadian Arctic region and arrive at Barrow the majority of trajectories had originated over the northern Canadian, Greenland and Central Arctic territories. From one side, some of them arrived at Barrow from the direction of the Prudhoe Bay industrial area, and hence may carry out a signature of the regional industrial pollution. Prudhoe Bay is located to east of Barrow. Its emissions could be relatively well represented if the surface wind direction of 110°±35° is considered. We should note also that in the same time this industrial area is located in the "clean sector" for Barrow's measurements. From another side, Lowenthal et al., 1997 using air mass back trajectories reported that during collection of aerosol samples at Dye 3, Greenland, the North America continent (in particular, the east coast)

as well as Europe were identified as the source regions. The occurrence of such transport from the North America to Greenland is higher during fall and lower in winter (*Davidson et al., 1993*). On average, the developed cyclone systems pass the Northern Atlantic areas once-twice per week (*Whittaker and Horn, 1981*). The probability of removal along main tracks of the cyclones in the North Atlantic is higher during winter in comparison with other seasons (Whittaker and Horn; 1984; Hakim G. & McMurdie L., personal communication). Therefore, there is a likelihood that the relatively undiluted air parcels, if an intense removal does not occur, could reach the Canadian Arctic region initially following the main cyclone' pathways.

Using 10-day trajectories at 0.5 km we divided all elevated events (180 cases) within the Canadian Arctic region into two groups to investigate contribution of two mentioned above existing situations. Cases showing transport from the sector of 110°±35° were attributed to the Prudhoe Bay's category. We found that almost 30% (51 from 180 σ_{sp} elevated cases) of these trajectories possibly could carry out the Prudhoe Bay emissions signature. The rest corresponds to the long-range transport cases of the Canadian Arctic region. This distribution varies throughout the year reaching the maximum of transport occurrence from Prudhoe Bay during August-October - 42-53%, respectively, and it is the lowest - less than 10% - during March-April.

In the same manner, the low 10% of σ_{sp} were analyzed. For the Eurasian region during summer the lower number of elevated events corresponds with the higher number of lowered events during the same time of the year. The higher probability of the lowered events' occurrence for the Eurasian region is during summer - up to 26 and 48% - if 0.5 and 1.5 km trajectories are considered respectively. The North Pacific region has a controversial distribution if both altitudes are used. Throughout the year, the probability is on average of 31% if 1.5-km trajectories are applied, and it is reduced by factor of two for the low altitude. The highest probability of 75% is during February and an average of 43% is during winter-spring.

To see if the similarities in percentage of the event distribution exist, the rest 80% of σ_{sp} were tested as well as percentage of occurrence of elevated and lowered events with the rest of the data were compared. It showed that distributions for these 3 groups (elevated, lowered and the rest) are different and is not proportional. Finally, we should note that the use of trajectories at different altitudes to explain the specific events (elevated and lowered) based on the surface measurement provides different result in the comparison with the average concentrations of species. Therefore, we assume it will be more reasonably to apply the lower level trajectories to explain surface

measurements and then in the same time the check of flow consistence at both altitudes will be important for correct assignment of the particular specific event to the source region.

3.5. *TWO COMPONENT CORRELATION ANALYSIS*

At the first step the preliminary two component analyses of the entire YLP dataset without division by source regions had been performed. This analysis revealed that there is a strong (CH_4 vs. CO_2 and CH_4 vs. O_3) and fair (CH_4 vs. LogCN, CH_4 vs. LogBS, O_3 vs. CO_2, O_3 vs. LogBS, O_3 vs. LogCN, and LogBS vs. LogCN) statistically significant correlation which is observed during some periods. We found similar tendency and in the NLP dataset. To study more detail about relationship between species, this dataset was divided into separate groups of pairs of chemical species by season and month for each source region. We should note that very often the relationships between species could be hidden in the larger size dataset, but they will be revealed in the smaller datasets (i.e. re-arranged for the shorter time periods). We studied 10 possible different combinations of pairs of species. In each pair for each species we performed the test on the normality of the distribution and calculated the descriptive statistics. Depending on the calculated variances for the groups we performed the t-, Welch-, Fisher-tests to compare calculated test's values with the critical values in order to be sure that differences between species are significant. Then we calculated a correlation coefficient for each pair and tested its statistical significance at 90…99.8% confidence levels. For further analysis, we used only fair ($\geq|0.40|$) and 95% and better statistically significant correlation coefficients.

For visual inspection of the correlation between species the matrix scatter plots were produces for each source region by month. An example for the Eurasian region (September) is presented in Figure 4. As shown in Tables 4 and 5, each monthly record consists of the coefficient's magnitude, number of the pairs of cases used to calculate it and the statistical significance of coefficient (shown in brackets). If the correlation coefficient was less than an absolute value of 0.40 than we looked on the prevailing tendency in the correlation between species instead of the concrete magnitude. The sign "o" was used to underline that the correlation is very weak ($\leq|0.20|$), "+" - if species are positively, and "-" – negatively correlated. The "no source" group was also analyzed to evaluate how differ the chemical characteristics of trajectories arrived from the identified source regions with the rest of trajectories.

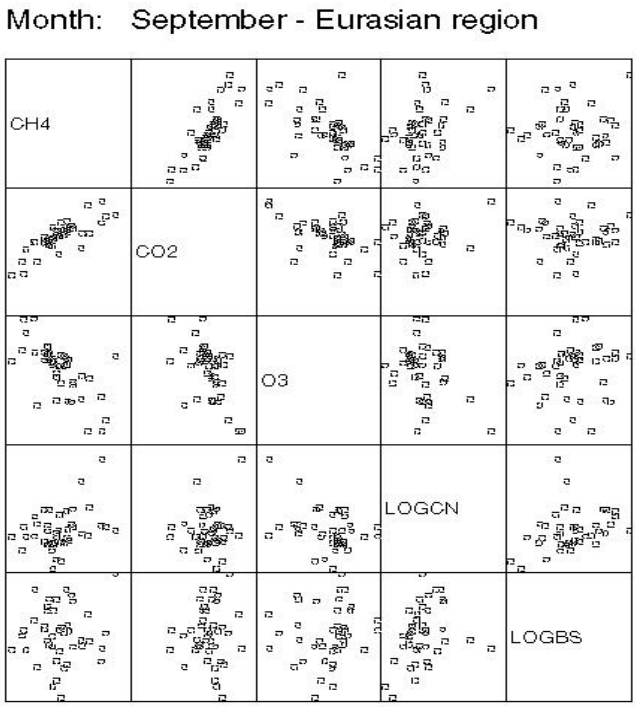

Figure 4. Matrix scatter plot of species vs. species for the Eurasian region during September.

Month	***No source***	***Eurasian***	***North Pacific***	***Canadian Arctic***
Jan	0.94 (24/99.8)	0.87 (46/99.8)	0.93 (16/99)	0.86 (143/99.8)
Feb	0.87 (68/99.8)	0.75 (51/99.8)	0.92 (32/99.8)	0.70 (111/99.8)
Mar	0.91 (52/99.8)	0.85 (60/99.8)	0.94 (21/99.8)	0.90 (86/99.8)
Apr	0.81 (83/99.8)	0.92 (40/99.8)	0.91 (37/99.8)	0.95 (197/99.8)
May	0.96 (63/99.8)	0.97 (19/99.8)	0.9 (43/99.8)	0.95 (221/99.8)
Jun	0.59 (58/99.8)	0.87 (15/99.8)	+	0.86 (112/99.8)
Jul	0.45 (67/99.8)	+	+	+
Aug	0.43 (73/99.8)	0.63 (38/99.8)	0.50 (40/99)	0.69 (62/99.8)
Sep	0.76 (72/99.8)	0.78 (33/99.8)	0.81 (24/99.8)	0.80 (66/99.8)
Oct	0.62 (86/99.8)	0.67 (32/99.8)	0.51 (24/95)	0.65 (139/99.8)
Nov	0.85 (80/99.8)	0.68 (45/99.8)	+	0.85 (167/99.8)
Dec	0.89 (64/99.8)	0.84 (81/99.8)	0.95 (14/99)	0.82 (164/99.8)

Table 4. Monthly correlation between methane and carbon dioxide by source region.

A positive correlation was always identified between CH_4 and CO_2 throughout the year for all trajectories (Table 4). It is very strong at 99.8% confidence level for all northern source regions (Eurasian and Canadian Arctic) during all months except July (less than 0.4). Similar results were previously reported for the spring Arctic haze (*Conway and Steele, 1989*). For the North Pacific region, the positive strong correlation could be identified during winter (99% confidence level) and

spring (99.8% confidence level) and this correlation is weaker during summer and fall. It is well known that both CH_4 and CO_2 have similar seasonal cycle with a minimum occurred in summer. This is related to chemical reactions of hydroxyl radicals with CH_4, destruction of CO_2 due to photosynthesis, and changes in flow patterns from the source regions. The weakening of the correlation between these two species during summer is associated with the larger contribution of CH_4 sources in tundra in comparison with CO_2.

Ozone is characterized by negative correlation with many studied species. The anti-correlation was identified between CH_4 and O_3 for all source regions except during spring when it is very weak (Table 5). This correlation is fear and strong at 99.8% confidence level for the northern source regions during fall and winter, and for the North Pacific regions during summer. Ozone is fairly negatively correlated at 98% confidence level with σ_{sp} during November-February for the trajectories showing transport from the North Pacific and weakly positively during February-March for the Eurasian region. Although throughout the year O_3 is negatively correlated with NC_{asl}, there are transitional periods starting in March and June when correlation switches signs from negative to positive and again back. Ozone is also fairly negatively correlated with CO_2 during November-January for all source regions and positively correlated during February-March for the Eurasian region.

Month	***No source***	***Eurasian***	***North Pacific***	***Canadian Arctic***
Jan	-0.45 (28/95)	-0.62 (44/99.8)	-0.69 (16/98)	-0.70 (147/99.8)
Feb	**o**	**o**	-0.73 (36/99.8)	-
Mar	**o**	**o**	**o**	**o**
Apr	**o**	**o**	**o**	**o**
May	**o**	**o**	**o**	**o**
Jun	**o**	-	-0.61 (38/99.8)	-
Jul	**o**	-	-0.57 (42/99.8)	-0.72 (73/99.8)
Aug	-	-	-0.65 (42/99.8)	-
Sep	-	-0.7 (34/99.8)	-0.57 (24/98)	-0.62 (81/99.8)
Oct	-0.42 (90/99.8)	-	-	-0.58 (146/99.8)
Nov	-0.69 (87/99.8)	-0.73 (50/99.8)	**o**	-0.53 (186/99.8)
Dec	-0.72/99.8)	-0.49 (85/99.8)	-	-0.69 (168/99.8)

Table 5. Monthly correlation between methane and ozone by source region.

The positive weak and in some individual months fear correlation between CH_4 and NC_{asl} was identified throughout the year for all source regions. Only a case of weak negative correlation was found for the North Pacific region (# pairs of species is equal 13 with R=-0.34 at less than 80%

confidence level). Although CH_4 and σ_{sp} are positively correlated throughout the year, there are two months - May and October - when they are negatively correlated for all trajectories arriving from different source regions with the transitional periods started in March and September. A positive correlation between CO_2 and σ_{sp} was identified for January-February for the Eurasian and North Pacific regions with the transitional periods starting in March and December. The correlation between NC_{asl} and CO_2 has a negative sign during February-April for the trajectories arriving from the Eurasian region. NC_{asl} and σ_{sp} are fairly positively correlated during late spring-summer for the Eurasian region and during July-September and November-March for the North Pacific region at 95% and higher confidence level. We should note that the spring period of transition is associated with the observed during this time the Arctic haze phenomenon. The fall-early winter reflect the beginning of the pollution gradual accumulation in the Arctic Basin pool as well as the partial stabilization of the process in the high arctic regions in the comparison with mid-latitudes.

3.6. *INFLUENCE OF THE PRUDHOE BAY INDUSTRIAL AREA ON BARROW'S RECORDS*

Prudhoe Bay Industrial Area (PBIA) is well known oil-developing region, which is located near the shore of the Arctic Ocean. It is situated approximately 300 km to the east-southeast of Barrow town at 110°. All facilities used to extract and transport oil cover approximately 2500 km^2 of the Alaskan arctic coastal plain. Previous work (*Jaffe et al., 1991; Jaffe et al., 1995; Brooks et al., 1997*) showed that the NO_x , CO_2, CH_4 and black carbon from this region are transported to the Barrow observatory when the surface winds are from the east. In particular, these studies were related to consideration of the "specific events", i.e. when measured concentrations at Barrow were relatively high. The question we stated in this study: what is the influence of the Prudhoe Bay industrial emissions on the Barrow data records?

To investigate the PBIA's influence on Barrow's records we considered only trajectories which crossed the Canadian Arctic region and arrived at Barrow at altitude of 0.5 km . We divided these trajectories (from NLP dataset) into two groups based on the wind direction sector. First, trajectories arrived at Barrow from the sector of 110°±35°, i.e. from the Prudhoe Bay industrial area. Second, trajectories came from all other directions, i.e. from the Rest of the Canadian Arctic (RCA) region. Then, for these two groups (PBIA and RCA) we calculated and compared average monthly and yearly concentration of species and performed two component correlation analyses.

Comparison of species' concentrations between these two groups revealed that there is a clear indication of aerosols' importance on the Barrow's records if the surface wind direction is from PBIA. Calculated average yearly concentration of species, standard deviation and number of cases used to calculate statistics for both groups are shown in Table 6.

Species	***Prudhoe Bay industrial area***	***Rest Canadian Arctic***	***SS at 95% cl***
CH_4	1789.10±38.99 (294)	**1798.07**±35.64 (1037)	Y
CO_2	355.15±6.76 (325)	**356.00**±6.48 (1159)	Y
O_3	26.48±8.83 (332)	**27.29**±9.50 (1219)	Y
Log BS	**-5.24**±0.49 (345)	-5.25±0.47 (1259)	Y
Log CN	**2.47**±0.43 (345)	2.24±0.45 (1259)	Y

Table 6. Average concentration of species, standard deviation and number of cases to calculate statistics for PBIA and RCA groups ("Y" or "N" shows the statistical significance of the calculated results at 95% confidence level).

As shown in Figure 5, in common, the higher NC_{asl} is the signature of PBIA. On average throughout the year it is higher for PBIA than RCA, except during March, which is well known as the beginning of the Arctic haze spring period and when the most of the anthropogenic pollutants transport occurs from the remote industrial sources of the Eurasian continent. During this time at all elevations we have the relatively high probability of transport from these regions. We used 95% confidence level for the mean NC_{asl} to show that this difference is well pronounced especially during July-February. Similar pattern exists for σ_{sp} showing on average higher concentration during May-December for PBIA. But during January-April it shows higher average concentration for RCA. The dominance of these two species in the PBIA transport is not surprise, because FA-PCA analysis revealed that these species are strongly correlated with the RSPF factor. Other species – CH_4, CO_2 and O_3 – showed on average higher concentrations for the RCA group throughout the year, except during April when they all dominate in the PBIA

Similar procedure to perform two component analyses was applied as described in chapter 3.5 of this paper. Similar pairs of species were investigated. Similar results as for the Canadian Arctic region were obtained. Analysis for two groups showed that there is no large statistically significant difference between species' correlations if PBIA and RCA are compared. We should

note that for the PBIA the correlation coefficient magnitude is higher for the following pairs of species: CH_4 vs. CO_2, Log CN vs. CO_2, Log CN vs. O_3.

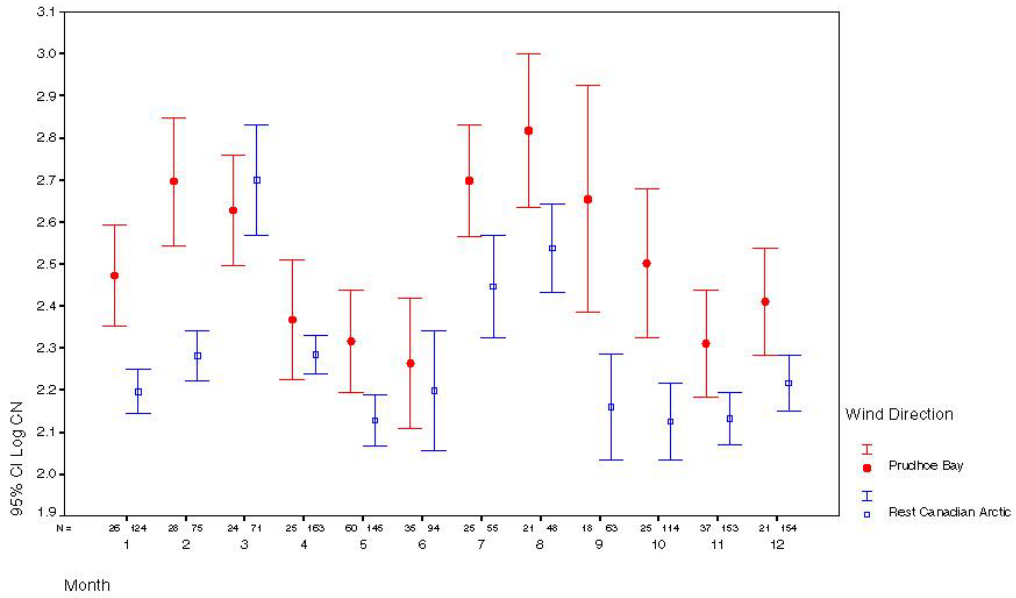

Figure 5. 95% confidence interval for the aerosol number concentration for Prudhoe Bay industrial area and Rest Canadian Arctic region vs. month (values, given along time axis, represent the number of points used to calculate average concentration).

3.7. *SPECIES' TRENDS BASED ON HOURLY AND FLASK DATA*

In this study we used the NLP dataset to estimate trends of species measured at Barrow. Previous studies in general are related to estimation of trends for species at the measurement site (*Dlugokencky et al., 1995; Ferguson and Rosson, 1991; Peterson and Komhyr, 1985; Polissar et al., 1999; Bodhaine et al., 1993*). In this study we evaluated and compared trends with respect to the studied source regions.

For this purpose, we considered concentration of species as a function of time: month and year. We have recognized that calculation of the trends for species is complicated due to natural variability and seasonal cycles. Therefore, first, we estimated trends for yearly average concentration of species by examining the residuals from the fitted line. Second, we calculated the average species' concentrations for each source region, in each month and in each year. Then we grouped them by months – all Januarys, Februarys, Marches, etc - to calculate linear trends as a function of a month. This permits us to investigate when during a year the contribution into records is the largest and smallest. We calculated magnitude of each monthly trend and estimated how much variance could be explained. All calculated monthly trends for source regions as well as trends between regions were tested on statistical significance at different confidence levels. We

applied similar procedure for flask CO, CO_2 and CH_4 data. Calculated in our study species' trends for source regions based on hourly and flask data are shown in Table 7. Values given in brackets show how much variance in time could be explained by given trend. The symbols "Y" or "N" show the statistical significance of the calculated trends at 95% confidence level in comparison with the "no source" region. CO_2 monthly trends based on hourly data is shown in Figure 6.

Species	***Source regions***						
	No Source	***Eurasian***	***SS***	***North Pacific***	***SS***	***Canadian Arctic***	***SS***
Trends based on NLP dataset (used hourly data)							
CH_4 (ppb/yr)	6.24 (0.83)	6.67 (0.92)	Y	7.62 (0.80)	Y	7.23 (0.85)	Y
CO_2 (ppm/yr)	1.35 (0.87)	1.35 (0.91)	N	1.25 (0.70)	Y	1.45 (0.91)	Y
Trends based on flask data							
CH_4 (ppb/yr)	5.73 (0.61)	7.14 (0.88)	Y	7.80 (0.66)	Y	8.08 (0.93)	Y
CO_2 (ppm/yr)	1.45 (0.82)	1.65 (0.91)	Y	1.73 (0.78)	Y	1.42 (0.98)	Y

Table 7. CH_4 and CO_2 trends vs. source regions based on hourly and flask data.

At the beginning of discussion, we should note that calculated trends for source regions depend on the length of the considered time period. I.e. in our study - on available isentropic trajectories (11 years), and hence possibly do not reflect long term trends for such species as ozone, aerosol scattering coefficient, σ_{sp}, and aerosol number concentration, NC_{asl}, which have a tendency to slow the rate of increase in recent years.

For CH_4, positive trends statistically significant at 95% confidence level were identified during November-July for all source regions. These trends could explain on average 80 % of variance in time. It should be noted that during August-October trends are not statistically significant at the same confidence level and they explain a smaller fraction of variance.

For CO_2, positive trends statistically significant at 95% confidence level were identified for all source regions. The positive trends of smaller magnitude are observed during July-October with the highest during winter - beginning of the spring (Figure 6). These monthly trends could explain between 90% of variance. The average trend of 1.36 ppmv/year was found at Barrow using NLP dataset. We should note that from all source regions the Canadian Arctic reflects the highest CO_2 trend (1.45 ppmv/year) in comparison with others. And the lowest trend - 1.25 ppmv/year – is for the North Pacific region during studied period.

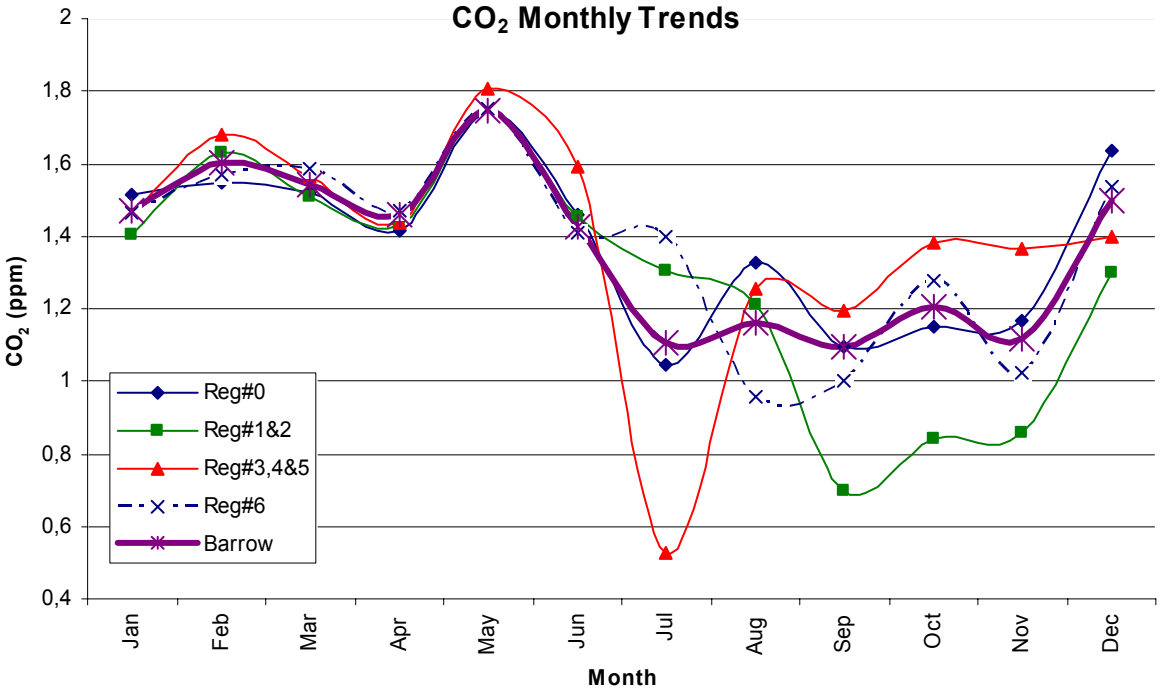

Figure 6. CO_2 monthly trends calculated using NLP dataset based on hourly data.

Trends of less than 1 ppmv/yr were found for the North Pacific region during July and for the Eurasian region during September-October. These trends explain only 65% of variance in time in comparison with other months and regions. It is interesting to note that there is a shift in occurrence of the lowest trend: in July for the North Pacific region vs. in September-October for the Eurasian region. As we mentioned already the visual inspection of the "no source" trajectories during summer showed, that the prevailing transport is from the south and southwest, i.e. from the middle latitude's areas of the Pacific Ocean. During fall, this type of trajectories shows transport from the northern latitude's areas. We could speculate that the lowest trends depend on: 1) the duration of the growing season when the uptake of CO_2 by vegetation will be the highest, and 2) the beginning of the heating season in the northern countries. In particular, this explains why during July trend of the "no source" region shows closer relationship with the North Pacific region, and in September - the Canadian Arctic region has the lowest trend as well as the Eurasian region.

In this study we used carbon dioxide emissions' database (*Andres et al., 1999; http://cdiac.esd.ornl.gov/*) and re-arranged available emission data for our geographical source regions for the studied period of 1985-1996 (Figure 7). It should be noted that we did not identify clear dependence of calculated trends vs. total CO_2 emissions from fossil-fuel consumption. Although the rate of these emissions increase per year is higher for the North Pacific region, the

total amount of emissions was still lower than for the Canadian Arctic. This situation has been changing since 1995 but in this study, the later years were not considered. We could speculate that this discrepancy is connected with the relatively long residence time of CO_2 and its uniform distribution in atmosphere, and possibly the change in total emissions would not be fast reflected in the trend's records.

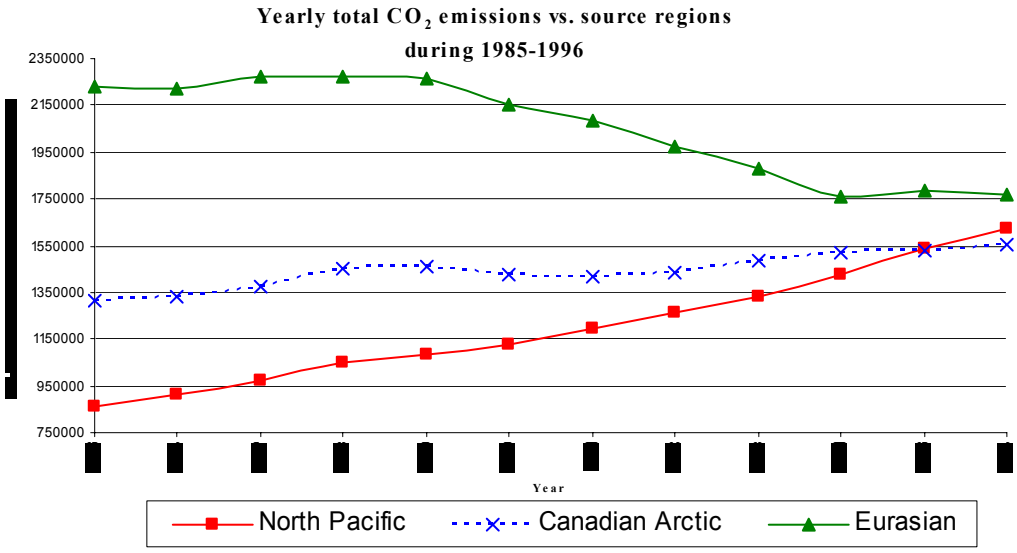

Figure 7. Yearly total CO_2 emissions from the fossil-fuel consumption vs. source regions during 1985-1996.

Although we did not obtained statistically significant trends for O_3, σ_{sp} and NC_{asl} by source regions, the following findings, which are valuable should be mentioned.

First, all source regions showed a tendency of occurrence of negative O_3 trends although with lower explanation of variance and lower statistical significance. Exception is the Eurasian region. In comparison with other source regions, this region has a long period (February-June) when the positive O_3 trends statistically significant at 90% confidence level had occurred. These trends vary from 0.22 to 0.73 ppbv/year with the higher values during April-May. We speculate that existence of such phenomenon could be explained in the following manner. We estimated that majority of calculated trajectories from the Eurasian region passed through the arctic territories at altitudes between 0.5-5 km. During this time in the northern high latitudes the frequency of tropopause folds, which could transfer air and trace gases from the stratosphere into the troposphere, is relatively high and the height of tropopause is lower in comparison with middle and

low latitudes (*Gruzdev and Sitnov, 1995; Blonsky and Speth, 1998; Elbern et al., 1998*). In the same time the photochemistry contribution is minimized and therefore ozone losses are small. Although anthropogenic sources of O_3 could contribute but not so significantly to change the common negative trend on opposite. There is another factor - possibility of O_3 intrusions from the stratosphere – it has related to intensity of tropopause folds mentioned above as well as depends on the Polar vortex's intensity (*Jou, 1985; Newman et al., 1996*). Support of stratospheric ozone intrusion contribution was obtained performing factor analysis in this study. Hence, for the Eurasian region, consideration of both O_3 sources – anthropogenic and stratospheric ozone intrusions - with the dominance of the latter is reflected in occurrence of the positive trends during this time.

Second, we looked for tendency in trends too, i.e. we considered also signs and magnitude of the trends, which explain smaller variances and are statistically significant at lower confidence levels. These tendencies could reflect possible common existing patterns, and could be compared with the previous studies applied for other time periods different from ours (1985-1995). In particular, for NC_{asl}, we identified a common tendency of positive trends during summer and winter, and tendency of negative trends during spring, which are well related to existing seasonal cycle. We should note that only during December for all source regions was observed an average positive trend of 0.045 $1/cm^3$/year. This trend is statistically significant at 95% confidence level and explains on average more than 55% of variance. For σ_{sp}, we identify a tendency of negative trends throughout the year for all source regions except during winter.

Although using flask data we still were able to calculate trends at Barrow, we run into problems when trends by source regions were considered. Because there are only a few flask measurements per month, the number of points used to calculate averages by source region dropped drastically. In particular, this complicates correct calculation for the North Pacific region, where the number of measurements assigned to trajectories is the lowest. This also influenced the estimation of the statistical significance for the obtained trends due to small number of the points. Therefore, for more than half of the months in this region we were not able to obtain statistically significant trends using flask data, although NLP dataset constructed based on hourly measurement gave reasonable results. Our calculated CH_4 and CO_2 trends at Barrow based on flask data produced slightly higher values than based on hourly data. In particular, during studied period, CH_4 trend of 6.96 ppbv/year was obtained, if hourly data were used and 7.43 ppbv/year, if flask data were considered. Similarly, the CO_2 trends of 1.36 and 1.48 ppmv/year were calculated when hourly and flask data were considered, respectively.

As well as hourly data, CO_2 and CH_4 flask data showed positive trends for all source regions and majority of these monthly trends are statistically significant at 95% confidence level. Although the negative CO trend (–2.3 ppbv/year) statistically significant at 95% confidence level was identified at Barrow using flask data for 1988-1996, we did not obtain statistically significant results considering the source regions separately. This negative trend is well known due to continuous decrease in the total anthropogenic emissions (*Novelli et al., 1998*). All source regions showed the tendency of negative trends throughout the year, except the Canadian Arctic region during June-August. It reflected the positive trends of 1.1-1.5 ppbv/year during these months, which we assumed are related to emissions from the Prudhoe Bay industrial area. To test this assumption we analyzed all (24) cases showed trajectories arriving from the Canadian Arctic region. We divided cases into two subgroups based on wind direction measured at surface: a) transport from the Prudhoe Bay industrial area (110°±35°) and b) transport from the rest of directions for the Canadian Arctic region. Finally, the average monthly CO concentrations for groups were calculated as shown in Table 8. We found that during summer on average the CO concentration is higher if an air mass arrived from the regional industrial area.

Cases Months	***Prudhoe Bay industrial area***			***Rest Canadian Arctic***			***Canadian Arctic region***		
	Avg	StD	#	Mean	StD	#	Mean	StD	#
Jun	121.31	25.20	6	113.17	6.07	4	118.06	19.56	10
Jul	102.91	32.89	4	100.24	11.12	4	101.57	22.78	8
Aug	97.92	0.53	2	90.63	10.65	4	93.06	9.07	6
Summer	111.28	26.39	12	101.34	12.96	12	106.31	20.96	24

Table 8. CO characteristics for groups (average, standard deviation, and number of cases) based on the Canadian Arctic trajectories.

Finally, we should comment that the use of flask data to calculate species' trends at the measurement site would be more valuable if the estimation of global background trends is a goal of the study. From another side, the use of original hourly data is more appropriate if the trends of species will be related to different geographical source regions.

3.8. *FACTOR ANALYSIS*

The main purpose of the factor analysis (FA) is to reveal the underlying structure, which presumably exists within a set of multivariate observations. Such structure could be expressed as a pattern of covariance, variances or correlations between variables and similarities between observations (*Davis, 1986*). The main problem represented in factor analysis is solved extracting

eigenvectors and eigenvalues from a square matrix produced by multiplying of original data matrix by its transpose (*Dillon and Goldstein, 1984*). Analysis transforms the original dataset into a linear combination, which represents relationship between original variables.

For FA as an extraction method we used the principal components analysis (PCA) method. This method is used to form uncorrelated linear combinations of the observed variables. The first component always explains maximum variance. All other successive components explain smaller portions of the variance and are all uncorrelated with each other. Two different approaches were used in our study. In the first approach, we did not rotate the extracted factors and therefore we analyzed un-rotated factor pattern matrixes. In the second approach, we used rotation methods to simplify the explanation of factor and variables, and we analyzed rotated factor pattern matrixes. We subsequently applied several rotation methods to check consistency and compare results obtained based on two approaches. In this study we used three different rotation methods (all orthogonal): varimax, quartimax, and equamax. The varimax method minimizes the number of variables that have high loadings on each factor, and therefore simplifies the interpretation of the factors. The quartimax method minimizes the number of factors needed to explain each variable, and therefore simplifies the interpretation of the observed variables. The equamax method is used to simplify the interpretation of both factors and variables. The role of variables is played by different chemical species in our study. For both approaches we analyzed the correlation between un-rotated/rotated principal components and dependent variables.

In our study the factor analysis – principal components analysis (FA-PCA) procedure was performed in several steps. Initially, datasets used in procedure were constructed based on two assumptions: a) the entire record at particular date was excluded if one of variables was missing in the record, and b) the variables in the record were replaced with a mean ("dummy values") if variables have missing values. Both assumptions are valuable, because the first provides factor's estimates based on real available data, and the second permits comparison if "dummy values" were incorporated in dataset.

At the beginning, the initial statistics (including magnitudes of communalities for each variable, number of factors, related to each factor the eigenvalues and percentage of explained variance by each eigenvalue, as well as cumulative percentage of explained variance) was produced. At the second step PCA extracted from dataset the most valuable number of factors (we considered for each factor the eigenvalue with magnitude of 1 and higher to be important for further consideration). Then the factor pattern matrix containing information about correlation between

variables and particular valuable factors, and loading plots showing the variable loadings with respect to factors were evaluated. At the end the final statistics only for important factors was produced with similar characteristics as at the beginning of procedure. The similar procedure, described above, was also applied for different rotation methods. In this case, additionally, we check information about the maximum number of iteration steps required for method to converge, and instead of un-rotated we analyzed the rotated factor pattern matrix.

FA-PCA procedure was performed for both NLP and YLP datasets. Then datasets were analyzed by month. A summary is presented in Tables 9 and 10. As an example, we included Figure 8 which shows the magnitude of eigenvalues, percentage of explained variance and cumulative percentage of explained variance by month. Analysis revealed the existence of two main similar factors in both YLP and NLP datasets. The first and second eigenvalues are larger than 1 and distinguishable from each other throughout the year (Table 9, Figure 8). Although on average the third eigenvalue has magnitude of less than 1, during spring it is above 1 (Figure 8). Both datasets showed that by using the first two factors it is possible to explain on average more than 65% of variance in the studied system (Table 9, Figure 8). Additional contribution of the third factor raises the cumulative percentage of explained variance above 85%. It should be noted that the application of the third factor is limited by the possibility of the eigenvalue to be distinguishable from the other eigenvalues only during spring.

Dataset	***NLP***			***YLP***		
Factor	***Factor #1***	***Factor #2***	***Factor #3***	***Factor #1***	***Factor #2***	***Factor #3***
Average magnitude of eigenvalue						
(excl dummy values)	2.21	1.22	0.84	2.22	1.19	0.84
(incl dummy values)	2.04	1.21	0.86	2.00	1.14	0.86
Average explained variance (in %)						
(excl dummy values)	44.5	23.7	16.8	44.2	24.4	16.8
(incl dummy values)	40.1	22.7	17.2	40.7	24.2	17.2

Table 9. Average magnitude of eigenvalues and percentage of average explained variance vs. different factors for NLP and YLP datasets including or excluding dummy values.

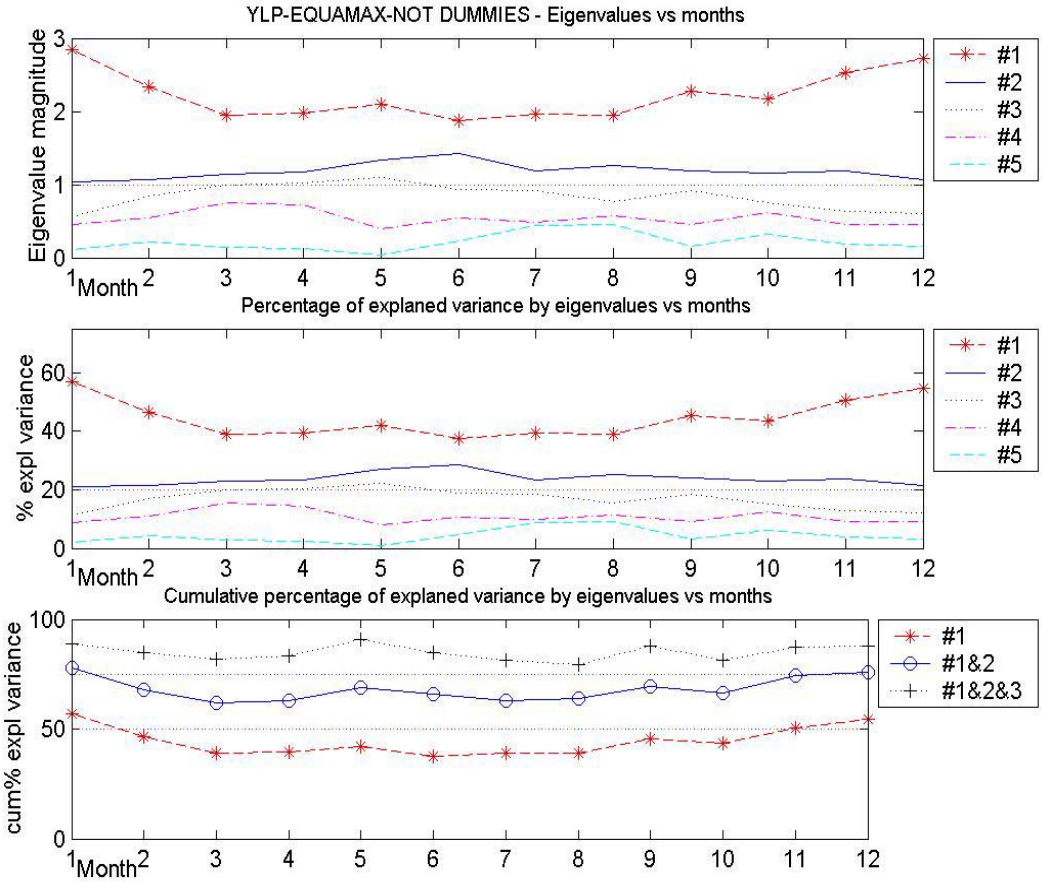

Figure 8. Eigenvalues, percentage of explained variance and cumulative percentage of explained variance by eigenvalues vs. month (case: YLP dataset, no dummy values, equamax rotation).

The first factor reflects higher correlation with the carbon group species represented by CH_4 and CO_2. Both species have relatively long residence time in the atmosphere (about 5-7 years for CO2 (*Warneck, 1988; Houghton, 1995*) and about 9-12.5 years (*Slinn, 1988; Harris et al., 1992*)) and during last decades were mostly accumulated due to anthropogenic contribution. The long residence time implies that both species are approximately conserved during long range transport from the remote geographical regions. Both species are also positively highly correlated between each other (*Conway and Steel, 1989; Jaffe et al., 1995*). We called it the "global hemispheric scale pollution factor" (GHSPF). The second factor reflects higher correlation with NC_{asl} and σ_{sp}. Both have relatively low residence time -order of several days to several months (*Warneck, 1988*) - in the comparison with the first factor and more likely could be assigned to "regional scale pollution factor" (RSPF). Only during spring the third factor emerged separately which is characterized by high (>0.9) correlation of O_3 with this factor. We called it the "stratospheric ozone intrusions

factor" (SOIF). The explanation of this pattern lies in the following two facts. First, during this time of the year within the high northern latitudes there is a high probability of air intrusions from the stratosphere into troposphere (*Chatfield and Harrison, 1977; Gregory et al., 1992*). Second, observations show that the troposphere represents a well-mixed layer in the Alaska Arctic, i.e. there is high probability of faster downward transport to boundary layer (*Strunin et al., 1997; Wessel et al., 1998*).

Dataset	***NLP***				***YLP***			
Factor	***GHSPF***		***RSPF***		***GHSPF***		***RSPF***	
Species / ***Rotation method***	***CH_4***	***CO_2***	***Log BS***	***Log CN***	***CH_4***	***CO_2***	***Log BS***	***Log CN***
(excl dummy values) Unrotated	0.89	0.76	0.62	0.52	0.87	0.72	0.61	0.47
Varimax	0.87	0.81	0.57	0.67	0.89	0.83	0.70	0.62
Equamax	0.87	0.81	0.57	0.67	0.89	0.83	0.70	0.62
Quartimax	0.87	0.81	0.58	0.66	0.89	0.82	0.60	0.53
(incl dummy values) Unrotated	0.85	0.70	0.67	0.49	0.81	0.67	0.45	0.43

Table 10. Average correlation coefficients between factors and species applying different rotation methods for NLP and YLP datasets including or excluding dummy values.

As an example, we included Figure 9, which shows the correlation of different species with factors reflecting the dominance of particular groups of species by month. A summary shown in Table 10 represent the correlation coefficient between species and the first two factors (GHSPF and RSPF) obtained by applying different rotation methods and using different datasets. The values shown in the table are calculated averages based on monthly magnitudes of correlation coefficients. All weak correlations of species (less than ±0.20) with factors were omitted, hence, we see that both factors are strongly correlated only with a particular group of species. Special attention should be paid to ozone (not included in table) which had showed on average a fair negative correlation of -0.43 with the GHSPF factor. In particular, we found the correlation coefficient between GHSPF and O_3 is –0.40 and –0.46 for NLP and YLP datasets respectively. We should mention that the nature of ozone is more complicated, especially in the Arctic regions, where role of sources is played by: a) intrusions from the stratosphere, b) tropospheric photochemistry (NO_x and HC) and c) anthropogenic sources. As we mentioned before we did not identify a statistically significant trend for O_3 in comparison with CH_4 and CO_2 in our study. We could speculate that O_3 is related to

probable sources on a local scale at Barrow, but it is not related to the mentioned factors, except during spring when it emerges as a separate factor OSIF.

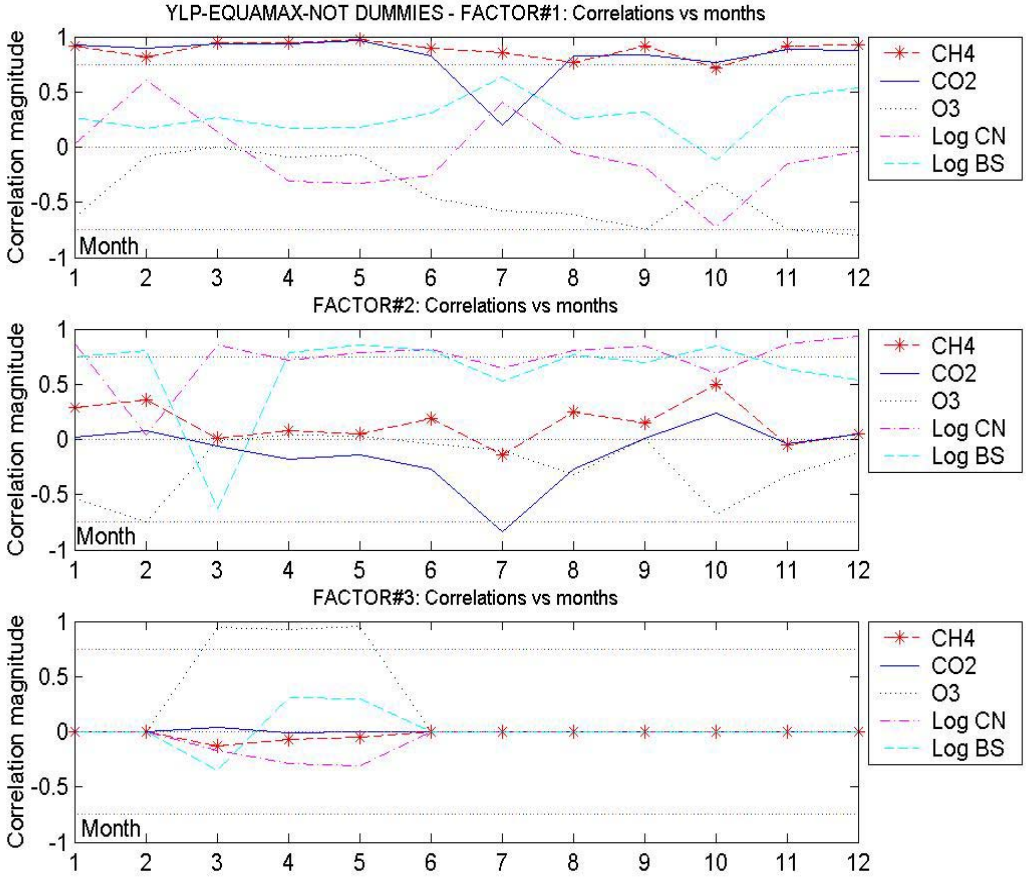

Figure 9. Correlation coefficients between species and factors vs. month (case: YLP dataset, no dummy values, equamax rotation).

An occurrence of interesting similar pattern in all datasets – weak correlation of CO2 with GHSPF and strong negative correlation with RSPF during July - let us speculate that during this time of the year CO_2 concentration has a local nature. In fact in the Northern Hemisphere during summer (at Barrow - July) there is a seasonal decline in CO_2 largely due to photosynthesis (*Keeling and Whorf, 1994*).

As we see from Table 10 the incorporation of dummy values in datasets for FA-PCA analysis does not change significantly the magnitudes of species' correlation with factors. It should be mentioned also that if dummy values are not considered on average 258 and 389 records per month are used for FA-PCA analysis for NLP and YLP datasets respectively. If FA-PCA analysis is performed incorporating dummy values then the number of records increases by 23 and 45% per

month for NLP and YLP datasets respectively. Comparison results of YLP with NLP dataset showed that the similar first two factors (GHSPF and RSPF) also exist in NLP dataset formed by the same groups of species. Factor SOIF emerged during spring too, although it did not occur in April. It is interesting that at the same time O_3 has a positive strong correlation (0.64) with RSPF allowing us to speculate that there is a probability of regional sources of ozone (possibly Prudhoe Bay industrial area).

It should be kept in mind, that presumably all possible local pollution events were excluded from the YLP dataset to build the NLP dataset, and then to prepare dataset for FA-PCA procedure some records were also additionally excluded due to missing values for some variables. Although a smaller in the size the NLP dataset showed a similar pattern.

SUMMARY AND CONCLUSIONS

Backward isentropic trajectories arriving at Barrow, Alaska had been calculated for 1985-1996 using an isentropic trajectory model. Calculated trajectories were used to relate air transport patterns at Barrow to different possible source pollution regions using hourly (CH_4, CO_2, O_3, NC_{asl} and σ_{sp}) and flask (CH_4, CO_2, and CO) data records. Segregation of trajectories was used to group trajectories, assigned them into different source regions (European and Taymyr as Eurasian; East, West, and Central North Pacific as North Pacific; and Canadian Arctic) with the rest attributed to "no source" category. In this study we combined trajectories with the available chemical records to look into the relationship between species and trajectories showing transport from different regions, to examine the correlation between species and evaluate the dependence of variations in flow patterns vs. chemical species. We also combined trajectories with the available chemical records to look into the interspecies relationship, species trends vs. source regions, and possibility of the Prudhoe Bay industrial area influence into the Barrow's records.

The main results of our study are as follows:

1. The clear pattern of the Eurasian region predominance in the transport of the anthropogenic pollutants such as CO, CO_2 and CH_4 was identified and it is in a good agreement with σ_{sp} data for the same period. The North Pacific region shows the higher concentration of NC_{asl} in comparison with others, which is mostly due to larger contribution of natural than anthropogenic sources.
2. Although 5-day trajectories reflecting main flow patterns show similar results for average concentration of species, they are less useful for identification of the source regions if the elevated and lowered events are considered, and therefore, 10-day trajectories will be more appropriate.
3. Although the usage of the shorter duration trajectories (5 instead of 10-day) increase the number of trajectories assigned to "no source" group, it does not change significantly the distribution of average concentration of species throughout the source regions.
4. Similar conclusion could be made if trajectories at different altitudes are used for interpretation of chemical species. Therefore, we are able to keep the tracking of "more polluted" regions in comparison with others on a base of main average flow patterns.
5. A strong positive correlation was identified between CH_4 and CO_2 statistically significant at 99.8% confidence level for all trajectories arriving from different source regions throughout the year except July. A strong negative correlation was found between CH_4 and O_3

statistically significant at 99.8% confidence level for the trajectories associated with the transport from the northern source regions during September-January and from the North Pacific during winter and summer.

6. Transitional periods, when the sign of correlation between species changed on opposite, were identified. These periods exist for the following species: CH_4 vs. LogBS during March and September and O_3 vs. LogCN during March and June for all source regions; and CO_2 vs. LogBS during March and December for the Eurasian and North Pacific regions.
7. Detail analysis of species concentrations vs. trajectories arrived from the Prudhoe Bay's direction using the Canadian Arctic region trajectories showed the predominance of the aerosol species – aerosol scattering coefficient, σ_{sp} and aerosols number concentration - as the signature of the regional scale influence on the Barrow's records.
8. The positive statistically significant trends for CO_2 and CH_4 were identified for all source regions, with an average trend of 1.36 ppmv/year and 6.96 ppbv/year at Barrow, respectively.
9. Although in general O_3 is characterized by negative trends, there are the positive trends during February-June for the Eurasian region (with the highest magnitude of 0.22-0.73 ppbv/year during April-May), which are supposedly is a result of the stratospheric ozone's intrusions.
10. In this study, using 1985-1995 data, we did not obtain certain statistically significant trends for σ_{sp} and NC_{asl} vs. source regions.
11. In general, there is an average negative CO trend of –2.3 ppbv/year at Barrow, although the summer is characterized by positive trends of 1.1 -1.5 ppbv/year for trajectories arrived through the Canadian Arctic region. It is also should be noted that the concentration of CO is on average higher, if trajectories arrived from the direction of the Prudhoe Bay industrial area.
12. Factor analysis revealed the existence of several factors in the datasets. There are two major factors – global hemispheric scale pollution factor (GHSPF) and regional scale pollution factor (RSPF) – which represent the contribution of the carbon and aerosol species throughout the year. The third factor – stratospheric ozone intrusions factor (SOIF) – is reflected only during spring.

13. Although in this study we suggested that month-to-month and year-to-year flow variations might be reflected in the concentration of the species measured at Barrow, we did not obtain a clear pattern-explanation for all species.

At the end of the conclusion, we should mention that in this study we accounted several problems, which will require additional attention in the future studies. These problems are related to the complete and correct interpretation of chemical records on the basis of trajectories, and they are connected with the following issues:

1. accuracy of trajectory calculations for the time periods more than 5 days;
2. large divergence of trajectories at elevations of 0.5, 1.5 and 3 km for the same temporal term, showing atmospheric transport from the different source regions;
3. if trajectories ("mixed trajectories") on their way to Barrow crossed several source regions than they carry out a "chemical fingerprint" of several regions simultaneously,

therefore, these lead to difficulties in the correct assigning of trajectories to the particular source region of smaller geographical sizes, and hence will require a generalization.

The problems we mentioned would allowed us to speculate that the consideration of chemical species (average concentration and specific cases of the elevated and lowered concentrations) with respect to source regions must be accompanied by the subsequent calculation of trajectories into two steps. First, several trajectories at one altitude with the different geographical resolution should be calculated and presumable they need to be the closest to the surface or within the boundary layer. For example, it could be 1° x 1° latitude/longitude box around the site. Second, then the trajectories at several altitudes above the site need to be calculated in order to analyze the differences in the spatial flow patterns, i.e. are there cases, which may show a "chemical fingerprint" of several source regions. Third, if the higher temporal resolution meteorological data is used to calculate trajectories, it is the better. We believe that this approach could eliminate the assignment of the chemistry to unrelated source region, and hence to improve the interpretation of the chemical records.

We assume that the further studies would require a consideration of the additional locations with the similar measurement programs to support the main conclusions of this study, for example, the Alert site in the Canadian Arctic.

ACKNOWLEDGMENTS

Support for this research has come from the NOAA through the Cooperative Institute for Arctic Research (CIFAR) and Joint Institute for Study of the Atmosphere and Ocean (JISAO, Cooperative agreement NA 67RJ0155). This publication is funded by the Joint Institute for the Study of the Atmosphere and Ocean (JISAO) under NOAA Cooperative Agreement. The views expressed herein are those of the authors and do not necessary reflect the views of NOAA or any of its sub-agencies. The computer facilities of National Center for Atmospheric Research (NCAR, Boulder, Colorado), Arctic Region Supercomputing Center (ARSC, Fairbanks, Alaska), Atmospheric Sciences Department of the University of Washington (Seattle, Washington), Danish Meteorological Institute (Copenhagen, Denmark) have been used extensively in this work. This work was supported in part by a grant of HPC time from the Arctic Region Supercomputing Center.

Authors acknowledge the National Oceanic and Atmospheric Administration (NOAA), Climate Monitoring and Diagnostics Laboratory (CMDL), Carbon Cycle, Aerosols and Ozone Groups for providing access to species hourly and flask measurements at Barrow.

Thanks to Glenn Shaw and Jennifer Kelley (Geophysical Institute, University of Alaska Fairbanks); Gregory Hakim, Lynn McMurdie, Robert Kotchenruther, Ulrike Dusek, Sungsu Park (Atmospheric Sciences Department, University of Washington) for constructive discussions and comments. Thanks to Robert Huebert, Dennis Fielding and Roger Edberg (ARSC), David Warren and Harry Edman (UW), DMI's UNIX & PC Computer Support Services for computer advice.

REFERENCES

Andres, R.J., D.J. Fielding, G. Marland, T.A. Boden, and N. Kumar. (1999): Carbon dioxide emissions from fossil-fuel use, 1751-1950. Tellus 51B, pp. 759-765.

Blonsky S. and Speth P., 1998: An algorithm to detect tropopause folds from ozone soundings. Meteorologische Zeitschrift, 7(4), pp. 153-162.

Bodhaine, Barry A. Dutton, Ellsworth G. (1993) A long-term decrease in Arctic haze at Barrow, Alaska. Geophysical Research Letters, 20, 947-950.

Bodhaine, Barry A. (1995) Aerosol absorption measurements at Barrow, Mauna Loa and the South Pole. Journal of Geophysical Research, 100, 8967-8975.

Bridgman, H. A. Schnell, R. C. Kahl, J. D. Herbert, G. A. Joranger, E. (1989) A major haze event near Point Barrow, Alaska: analysis of probable source regions and transport pathways. Atmospheric Environment, 23, 2537-2549.

Bridgman, H. A., Bodhaine, B.A. (1994) On the frequency of long-range transport events at Point Barrow, Alaska, 1983-1992, Atmospheric Environment, 28, 3537-3549.

Brooks S.R., Crawford T.L. and Oechel W.C. (1997) Measurements of Carbon Dioxide Emissions Plumes from Prudhoe Bay, Alaska Oil Fields. J. Atmos. Chem. 27, 197-207.

Browell, E. V. Butler, C. F. Kooi, S. A. Fenn, M. A Harriss, R. C. Gregory, G. L. (1992) Large-scale variability of ozone and aerosols in the summertime Arctic and sub-Arctic troposphere. Journal of Geophysical Research, 97, 16433-16450.

Chatfield R. and Harrison H., 1977: Tropospheric ozone, Part 2, Variations along a meridional band. Journal of Geophysical Research, 82(37), pp. 5969-5976.

Conway T.J. and L.P. Steele (1989) Carbon dioxide and Methane in the Arctic Atmosphere. Journal of Atmospheric Chemistry.

Conway, T.J., P.P. Tans, L.S. Waterman, K.W. Thoning, D.R. Kitzis, K.A. Masarie, and N. Zhang (1994) Evidence for interannual variability of the carbon cycle from the NOAA/CMDL global air sampling network. J. Geophys. Res., 99, 22831-22855.

Davidson, Cliff I. Jaffrezo, Jean-Luc Small, Mitchell J. Summers, Peter W. Olson, Marvin P. Borys, Randy D. (1993) Trajectory analysis of source regions influencing the south Greenland ice sheet during the Dye 3 gas and aerosolsampling program. Atmospheric Environment, 27A, 2739-2749.

Davis J.C., 1986: Statistics and data analysis in geology. 646 pp.

Dillon W.R., Goldstein M., 1984: Multivariate analysis: methods and applications. 587 pp.

Dlugokencky, E.J., L.P. Steele, P.M. Lang, and K.A. Masarie (1994) The growth rate and distribution of atmospheric methane. J. Geophys. Res., 99, 17,021-17,043.

Dlugokencky, E.J., Steele, L. P., Lang, P.M., Masarie, K.A. (1995) Atmospheric methane at Mauna Loa and Barrow observatories: presentation and analysis of in situ measurements. Journal of Geophysical Research, 100, 23103-23113.

Dorling, S.R. and Davies, T.D. (1995) Extending cluster analysis synoptic meteorology links to characterize chemical climates at six northwest European monitoring stations. Atmos. Environ. 29, 145-167.

Draxler, R.R. (1987) Sensitivity of a trajectory model to the spatial and temporal resolution of the meteorological data during CAPTEX. J.Clim. Appl. Meteorol. 26, 1577-1588.

Elbern H., Hendricks J., Ebel A., 1998: A climatology of tropopause folds by global analyses. Theoretical and Applied Climatology, 59(3-4), pp. 181-200.

Ferguson E.E. and Rosson R.M., 1991: Summary report 1991. National Oceanic and Atmospheric Administration, Environmental Research Laboratories, Climate Monitoring and Diagnostics Laboratory Reports, No. 20, 131 p.

Gregory, G.L., Anderson B.E., Warren L.S., Browell E.V., Bagwell D.R., Hudgins C.H. (1992) Tropospheric ozone and aerosol observations: the Alaskan Arctic. Journal of Geophysical Research, 97, 16451-16471, 1992.

Gruzdev A.N. and Sitnov S. A., 1995: Characteristics of intraannual variability of ozone vertical distribution derived from ozonesonde data. Izvestiya, Atmospheric and Oceanic Physics, 31(1), pp. 63-70.

Harris, J.M. and Kahl, J.D. (1990) A descriptive atmospheric transport climatology for Mauna Loa observatory, using clustered trajectories. J.Geophys.Res. 95,13651-13667.

Harris, J.M., Tans P.P., Dlugokencky E.J., Masarie K.A., Lang P.M, Whittlestone S., Steele L.P., (1992): Variations in atmospheric methane at Mauna Loa Observatory related to long-range transport. Journal of Geophysical Research, 6003-6010.

Harris, J.M. and Kahl, J.D. (1994) Analysis of 10-day isentropic flow patterns for Barrow, Alaska: 1985-1992. J.Geophys.Res. 99, 25845-25855.

Houghton R.A., 1995: Land-use change and the carbon cycle. Global change biology 1, pp. 275-287

Jaffe, D. A. ,Honrath, R. E. ,Herring, J. A. ,Li, S.-M. ,Kahl, J. D. (1991) Measurements of nitrogen oxides at Barrow, Alaska during spring: evidence for regional and Northern Hemispheric sources of pollution. Journal of Geophysical Research, 96, 7395-7405.

Jaffe, D. A., Honrath, R. E., Furness, D., Conway, T. J., Dlugokencky, E., Steele, L. P. (1995) A determination of the CH4, NOx and CO2 emissions from the Prudhoe Bay, Alaska Oil Development. Journal of Atmospheric Chemistry, 20, 213-227.

Jaffe, D.A., Mahura A.G., Kelley, J.A., Atkins J., Novelli P.C. and Merrill J.T. (1997a) Impact of Asian emissions on the remote North Pacific atmosphere: interpretation of CO data from Shemya, Guam, Midway and Mauna Loa. J.Geophys.Res, 102, 28627-28653.

Jaffe, D.A., Mahura, A.G., Andres, R.J. (1997b) Atmospheric transport pathways to Alaska from potential radionuclide sites in the former Soviet Union. UAF-ADEC research report, 71pp.

Jaffe, Dan ,Anderson, Theodore ,Covert, Dave ,Kotchenruther, Robert ,Trost, Barbara ,Danielson, Jen ,Simpson, William ,Berntsen, Terje ,Karlsdottir, Sigrun ,Blake, Donald ,Harris, Joyce ,Carmichael, Greg ,Uno, Itsushi (1999) Transport of Asian air pollution to North America. Geophysical Research Letters, 26, 711-714.

Jou B.J. 1985: Planetary wave breaking and ozone transport in the middle stratosphere: a numerical study. Papers in Meteorological Research, Taipei, Taiwan, 8(2), pp. 21-46.

Kahl, J.D. and Samson P.J. (1986) Uncertainties in trajectory calculations due to low resolution meteorological data. J. Clim. Appl. Meteor. 25, 1816-1831.

Kahl, J.D. (1996) On the prediction of trajectory model error. Atmos. Environ. 30, 2945-2957.

Keeling C.D. and Whorf T.P, 1994: Atmospheric CO2 from sites in the SIO air sampling network. In "Trends '93: A compendium of data on global change", pp. 16-26.

Li, Shao-Meng Winchester, John W. Kahl, Jonathan D. Oltmans, Samuel J. Schnell, Russell C. Sheridan, Patrick J. (1990) Arctic boundary layer ozone variations associated with nitrate, bromine, and meteorology: a case study. Journal of Geophysical Research, 95, 22433-22440.

Merrill, J.T., Bleck, R. And Avila, L. (1985) Modeling atmospheric transport to the Marshall Islands. J.Geophys.Res. 90, 12927-12936.

Merrill, J.T., Bleck, R. and Boudra, D.B. (1986) Techniques of Lagrangian trajectory analysis in isentropic coordinates. Monthly Weather Review 114, 571-581.

Miller, J.M. (1981) A five-year climatology of back trajectories from the Mauna Loa observatory, Hawaii. Atmos. Environ. 15, 1553-1558.

Newman P.A., Lait L.R., Schoeberl M.R., Seablom M., Coy L., Rood R., Swinbank R., Proffitt M., Loewenstien M., Podolske J.R., Elkins J.W., Webster C.R., May R.D., Fahey D.W., Dutton G.S., Chan K.R., 1996: Measurements of polar vortex air in the midlatitudes, Journal of Geophysical Research, 101(D8), pp. 12879-12891.

Novelli, P.C., K.A. Masarie, and P.M. Lang, 1998: Distributions and recent changes in carbon monoxide in the lower troposphere, J. Geophys. Res., 103, pp. 19,1015-19,033.

Oechel, W.C., Vourlitis, G.L., Hastings S.J., Bochkarev S.A. (1995) Change in Arctic CO2 flux over two decades: effects of climate change at Barrow, Alaska. Ecological Applications, 5, 846-855.

Oltmans, S. J., Levy, H.II (1994) Surface ozone measurements from a global network. Atmospheric Environment, 28, 9-24.

Peterson J.T. and Komhyr W.D., 1985: Atmospheric CO_2 measurements at Barrow, Alaska. Geophys. Monitoring for Climatic Change, Air Resources Lab./NOAA, Boulder, CO. IN: World Meteorological Organization, Geneva, Special Environmental Report No. 16, 1985, p. 76-80.

Polissar, A. V. Hopke, P. K. Paatero, P. Kaufmann, Y. J. Hall, D. K. Bodhaine, B. A. Dutton, E. G. Harris, J. M. (1999) The aerosol at Barrow, Alaska: long-term trends and source locations. Atmospheric Environment, 33, 2441-2458.

Polissar, A.V., P.K. Hopke, J.M. HARRIS, B.A. BODHAINE, and E.G. DUTTON. (1998) Source regions for atmospheric aerosol measured in the western Arctic. Journal of Aerosol Science, 29, S513-S514.

Shaw, Glenn E. (1991) Aerosol chemical components in Alaska air masses. 1: Aged pollution. Journal of Geophysical Research, 96, 22357-22368.

Slinn, W.G.N.,1988: A simple model for Junge's relationship between concentration fluctuations and residence times for tropospheric trace gases. Tellus 40B, pp. 229-232.

Stohl, A. (1998) Computation, Accuracy and Applications of Trajectories-A review and Bibliography. Atmospheric Environment, 32, 6, 947-966.

Strunin M.A., Postnov A.A., Mezrin M.Y.: 1997. Meteorological potential for contamination of arctic troposphere: boundary layer structure and turbulent diffusion characteristics. Atmospheric Research, 44(1-2), pp. 37-51.

Sturges W.T., Schnell R.C., Landsberger S., Oltmans S. J., Harris J. M., Li S.-M. (1993) Chemical and meteorological influences on surface ozone destruction at Barrow, Alaska, during spring 1989. Atmospheric Environment, 27A, 2851-2863.

Warneck P., 1988: Chemistry of the natural atmosphere.

Wessel S., Aoki S., Winkler P., Weller P., Herber A., Gernandt H., Schrems O.,1998: Tropospheric ozone depletion in polar regions: a comparison of observations in the Arctic and Antarctic. Tellus, Series B: Chemical and Physical Meteorology, 50B(1), pp. 34-50.

Whittaker L.M. and L.H. Horn (1984) Northern Hemisphere Extratropical Cyclone Activity for Four Mid-Season Months. Journal of Climatology, 4, 297-310.

Whittaker L.M. and L.H. Horn (1981) Geographical and Seasonal Distribution of North American Cyclogenesis, 1958-1977. Monthly Weather Review, 109, 2312-2322.

Zaizen, Yuji Okada, Kikuo Ikegami, Miwako Aoki, Teruo Sawa, Yousuke Nishio, Fumihiko Tachibana, Yoshihiro (1998) Size distribution of aerosols at Barrow in Alaska: a case study in spring. Polar Meteorology and Glaciology, 12, 40-48.

DANISH METEOROLOGICAL INSTITUTE

Scientific Reports

Scientific reports from the Danish Meteorological Institute cover a variety of geophysical fields, i.e. meteorology (including climatology), oceanography, subjects on air and sea pollution, geomagnetism, solar-terrestrial physics, and physics of the middle and upper atmosphere.

Reports in the series within the last five years:

No. 99-1
Henrik Feddersen: Project on prediction of climate variations on seasonel to interannual timescales (PROVOST) EU contract ENVA4-CT95-0109: DMI contribution to the final report: Statistical analysis and post-processing of uncoupled PROVOST simulations

No. 99-2
Wilhelm May: A time-slice experiment with the ECHAM4 A-GCM at high resolution: the experimental design and the assessment of climate change as compared to a greenhouse gas experiment with ECHAM4/OPYC at low resolution

No. 99-3
Niels Larsen et al.: European stratospheric monitoring stations in the Artic II: CEC Environment and Climate Programme Contract ENV4-CT95-0136. DMI Contributions to the project

No. 99-4
Alexander Baklanov: Parameterisation of the deposition processes and radioactive decay: a review and some preliminary results with the DERMA model

No. 99-5
Mette Dahl Mortensen: Non-linear high resolution inversion of radio occultation data

No. 99-6
Stig Syndergaard: Retrieval analysis and methodologies in atmospheric limb sounding using the GNSS radio occultation technique

No. 99-7
Jun She, Jacob Woge Nielsen: Operational wave forecasts over the Baltic and North Sea

No. 99-8
Henrik Feddersen: Monthly temperature forecasts for Denmark - statistical or dynamical?

No. 99-9
P. Thejll, K. Lassen: Solar forcing of the Northern hemisphere air temperature: new data

No. 99-10
Torben Stockflet Jørgensen, Aksel Walløe Hansen: Comment on "Variation of cosmic ray flux and global coverage - a missing link in solar-climate relationships" by Henrik Svensmark and Eigil Friis-Christensen

No. 99-11
Mette Dahl Meincke: Inversion methods for atmospheric profiling with GPS occultations

No. 99-12
Hans-Henrik Benzon; Laust Olsen; Per Høeg: Simulations of current density measurements with a Faraday Current Meter and a magnetometer

No. 00-01
Per Høeg; G. Leppelmeier: ACE - Atmosphere Climate Experiment

No. 00-02
Per Høeg: FACE-IT: Field-Aligned Current Experiment in the Ionosphere and Thermosphere

No. 00-03
Allan Gross: Surface ozone and tropospheric chemistry with applications to regional air quality modeling. PhD thesis

No. 00-04
Henrik Vedel: Conversion of WGS84 geometric heights to NWP model HIRLAM geopotential heights

No. 00-05
Jérôme Chenevez: Advection experiments with DMI-Hirlam-Tracer

No. 00-06
Niels Larsen: Polar stratospheric clouds microphysical and optical models

No. 00-07
Alix Rasmussen: "Uncertainty of meteorological parameters from DMI-HIRLAM"

No. 00-08
A.L. Morozova: Solar activity and Earth's weather. Effect of the forced atmospheric transparency changes on the troposphere temperature profile studied with atmospheric models

No. 00-09
Niels Larsen, Bjørn M. Knudsen, Michael Gauss, Giovanni Pitari: Effects from high-speed civil traffic aircraft emissions on polar stratospheric clouds

No. 00-10
Søren Andersen: Evaluation of SSM/I sea ice algorithms for use in the SAF on ocean and sea ice, July 2000

No. 00-11
Claus Petersen, Niels Woetmann Nielsen: Diagnosis of visibility in DMI-HIRLAM

No. 00-12
Erik Buch: A monograph on the physical oceanography of the Greenland waters

No. 00-13
M. Steffensen: Stability indices as indicators of lightning and thunder

No. 00-14
Bjarne Amstrup, Kristian S. Mogensen, Xiang-Yu Huang: Use of GPS observations in an optimum interpolation based data assimilation system

No. 00-15
Mads Hvid Nielsen: Dynamisk beskrivelse og hydrografisk klassifikation af den jyske kyststrøm

No. 00-16
Kristian S. Mogensen, Jess U. Jørgensen, Bjarne Amstrup, Xiaohua Yang and Xiang-Yu Huang: Towards an operational implementation of HIRLAM 3D-VAR at DMI

No. 00-17
Sattler, Kai; Huang, Xiang-Yu: Structure function characteristics for 2 meter temperature and relative humidity in different horizontal resolutions

No. 00-18
Niels Larsen, Ib Steen Mikkelsen, Bjørn M. Knudsen m.fl.: In-situ analysis of aerosols and gases in the polar stratosphere. A contribution to THESEO. Environment and climate research programme. Contract no. ENV4-CT97-0523. Final report

No. 00-19
Amstrup, Bjarne: EUCOS observing system experiments with the DMI HIRLAM optimum interpolation analysis and forecasting system

No. 01-01
V.O. Papitashvili, L.I. Gromova, V.A. Popov and O. Rasmussen: Northern polar cap magnetic activity index PCN: Effective area, universal time, seasonal, and solar cycle variations

No. 01-02
M.E. Gorbunov: Radioholographic methods for processing radio occultation data in multipath regions

No. 01-03
Niels Woetmann Nielsen; Claus Petersen: Calculation of wind gusts in DMI-HIRLAM

No. 01-04
Vladimir Penenko; Alexander Baklanov: Methods of sensitivity theory and inverse modeling for estimation of source parameter and risk/vulnerability areas

No. 01-05
Sergej Zilitinkevich; Alexander Baklanov; Jutta Rost; Ann-Sofi Smedman, Vasiliy Lykosov and Pierluigi Calanca: Diagnostic and prognostic equations for the depth of the stably stratified Ekman boundary layer

No. 01-06
Bjarne Amstrup: Impact of ATOVS AMSU-A radiance data in the DMI-HIRLAM 3D-Var analysis and forecasting system

No. 01-07
Sergej Zilitinkevich; Alexander Baklanov: Calculation of the height of stable boundary layers in operational models

No. 01-08
Vibeke Huess: Sea level variations in the North Sea – from tide gauges, altimetry and modelling

No. 01-09
Alexander Baklanov and Alexander Mahura: Atmospheric transport pathways, vulnerability and possible accidental consequences from nuclear risk sites: methodology for probabilistic atmospheric studies

No. 02-01
Bent Hansen Sass and Claus Petersen: Short range atmospheric forecasts using a nudging procedure to combine analyses of cloud and precipitation with a numerical forecast model

No. 02-02
Erik Buch: Present oceanographic conditions in Greenland waters

No. 02-03
Bjørn M. Knudsen, Signe B. Andersen and Allan Gross: Contribution of the Danish Meteorological Institute to the final report of SAMMOA. CEC contract EVK2-1999-00315: Spring-to.-autumn measurements and modelling of ozone and active species

No. 02-04
Nicolai Kliem: Numerical ocean and sea ice modelling: the area around Cape Farewell (Ph.D. thesis)

No. 02-05
Niels Woetmann Nielsen: The structure and dynamics of the atmospheric boundary layer

No. 02-06
Arne Skov Jensen, Hans-Henrik Benzon and Martin S. Lohmann: A new high resolution method for processing radio occultation data

No. 02-07
Per Høeg and Gottfried Kirchengast: ACE+: Atmosphere and Climate Explorer

No. 02-08
Rashpal Gill: SAR surface cover classification using distribution matching

No. 02-09
Kai Sattler, Jun She, Bent Hansen Sass, Leif Laursen, Lars Landberg, Morten Nielsen og Henning S. Christensen: Enhanced description of the wind climate in Denmark for determination of wind resources: final report for 1363/00-0020: Supported by the Danish Energy Authority

No. 02-10
Michael E. Gorbunov and Kent B. Lauritsen: Canonical transform methods for radio occultation data

No. 02-11
Kent B. Lauritsen and Martin S. Lohmann: Unfolding of radio occultation multipath behavior using phase models

No. 02-12
Rashpal Gill: SAR ice classification using fuzzy screening method

No. 02-13
Kai Sattler: Precipitation hindcasts of historical flood events

No. 02-14
Tina Christensen: Energetic electron precipitation studied by atmospheric x-rays

No. 02-15
Alexander Mahura and Alexander Baklanov: Probablistic analysis of atmospheric transport patterns from nuclear risk sites in Euro-Arctic Region

No. 02-16
A. Baklanov, A. Mahura, J.H. Sørensen, O. Rigina, R. Bergman: Methodology for risk analysis based on atmospheric dispersion modelling from nuclear risk sites

No. 02-17
A. Mahura, A. Baklanov, J.H. Sørensen, F. Parker, F. Novikov K. Brown, K. Compton: Probabilistic analysis of atmospheric transport and deposition patterns from nuclear risk sites in russian far east

No. 03-01
Hans-Henrik Benzon, Alan Steen Nielsen, Laust Olsen: An atmospheric wave optics propagator, theory and applications

No. 03-02
A.S. Jensen, M.S. Lohmann, H.-H. Benzon and A.S. Nielsen: Geometrical optics phase matching of radio occultation signals

No. 03-03
Bjarne Amstrup, Niels Woetmann Nielsen and Bent Hansen Sass: DMI-HIRLAM parallel tests with upstream and centered difference advection of the moisture variables for a summer and winter period in 2002

No. 03-04
Alexander Mahura, Dan Jaffe and Joyce Harris: Identification of sources and long term trends for pollutants in the Arctic using isentropic trajectory analysis